Progress in Oceanography 184 (2020) 102333

Contents lists available at ScienceDirect

Progress in Oceanography

journal homepage: www.elsevier.com/locate/pocean

Improved and extended tide gauge records for the British Isles leading to more consistent estimates of sea level rise and acceleration since 1958

P. Hogarth[a,b,*], C.W. Hughes[a,b], S.D.P. Williams[b], C. Wilson[b]

[a] University of Liverpool, United Kingdom
[b] National Oceanography Centre, Liverpool, United Kingdom

ARTICLE INFO

Keywords:
Sea level rise
Sea level acceleration
Mean sea level
Tide gauge
Time series analysis

ABSTRACT

This paper describes methods of obtaining improved estimates of long-term sea level trends for the British Isles. This is achieved by lengthening the sea level records where possible, then removing known sources of variability, and then further adjusting for datum errors that are revealed by the previous processes after verification using metadata from archived sources. Local sea level variability is accounted for using a tide and surge model. Far field variability is accounted for using a "common mode". This combination reduces the residual variability seen at tide gauges around the coast of the British Isles to the point that a number of previously unrecognised steps in individual records become apparent, permitting a higher level of quality control to be applied. A comprehensive data archaeology exercise was carried out which showed that these step-like errors are mostly coincident with recorded site-specific changes in instrumentation, and that in many cases the periodic tide gauge calibration records can be used to quantify these steps. A smaller number of steps are confirmed by "buddy-checking" against neighbouring tide gauges. After accounting for the observed steps, using levelling information where possible and an empirical fit otherwise, the records become significantly more consistent. The steps are not found to make a large difference to the trend and acceleration observed in UK sea level overall, but their correction results in much more consistent estimates of first order (Sea Level Rise) and second order (Sea Level Acceleration) trends over this 60-year period. We find a mean rate of sea level rise of 2.39 $\pm$ 0.27 mm yr^{-1}, and an acceleration of 0.058 $\pm$ 0.030 mm yr^{-2} between Jan. 1958 and Dec. 2018. The cleaner dataset also permits us to show more clearly that the variability other than that derived from local meteorology is indeed consistent around the UK, and relates to sea level changes along the eastern boundary of the North Atlantic.

1. Introduction

Our overall aim in this paper is to extend and improve the British Isles monthly Mean Sea Level (MSL) dataset, to begin to understand the sources of the observed variability in the improved dataset, and to quantify sea level trends and accelerations.

This paper significantly improves the sea level records: (1) by using results of a data archaeology exercise to extend the sea level data set where possible; (2) by making use of a barotropic model to remove much of the variability due to local meteorology; (3) by deriving and subtracting a common mode, representing variability from more distant sources. This results in much smoother residual data, in which steps due to data recording errors are more apparent, leading to (4) a further data archaeology exercise demonstrating that most of those steps are associated with known instrumentation changes, and that levelling and related data are available for most segments of data between steps, allowing them to be objectively adjusted. We also (5) adjust those segments for which such information is not available, so as to minimise the steps. Finally (6) it is shown that the resulting dataset is more consistent and results in improved estimates of trends and accelerations of sea level rise around the British Isles. We have selected a minimum of 20 years of valid data to derive SLR trends, and 50 years to derive acceleration.

The tide gauge network (Fig. 1) around the British Isles is a dense series of coastal sea level measurement sites situated on a shallow continental shelf sea on the Eastern boundary of the North Atlantic. The data from tide gauges installed around the British Isles and along the adjacent continental coast have been the subject of scientific study from the early 19th Century. More recent work has investigated sources of variability, allowing more refined estimates of Sea Level Rise (SLR) in the region (Rossiter, 1967; Thompson, 1980; Woodworth, 1987; Woodworth et al., 1999; Woodworth et al., 2009; Wahl et al., 2013;

* Corresponding author at: Floor 1, NOC, Joseph Proudman Building, 6 Brownlow Street, Liverpool L3 5DA, United Kingdom.
E-mail address: p.hogarth@liverpool.ac.uk (P. Hogarth).

https://doi.org/10.1016/j.pocean.2020.102333
Received 11 September 2019; Received in revised form 10 April 2020; Accepted 10 April 2020
Available online 17 April 2020

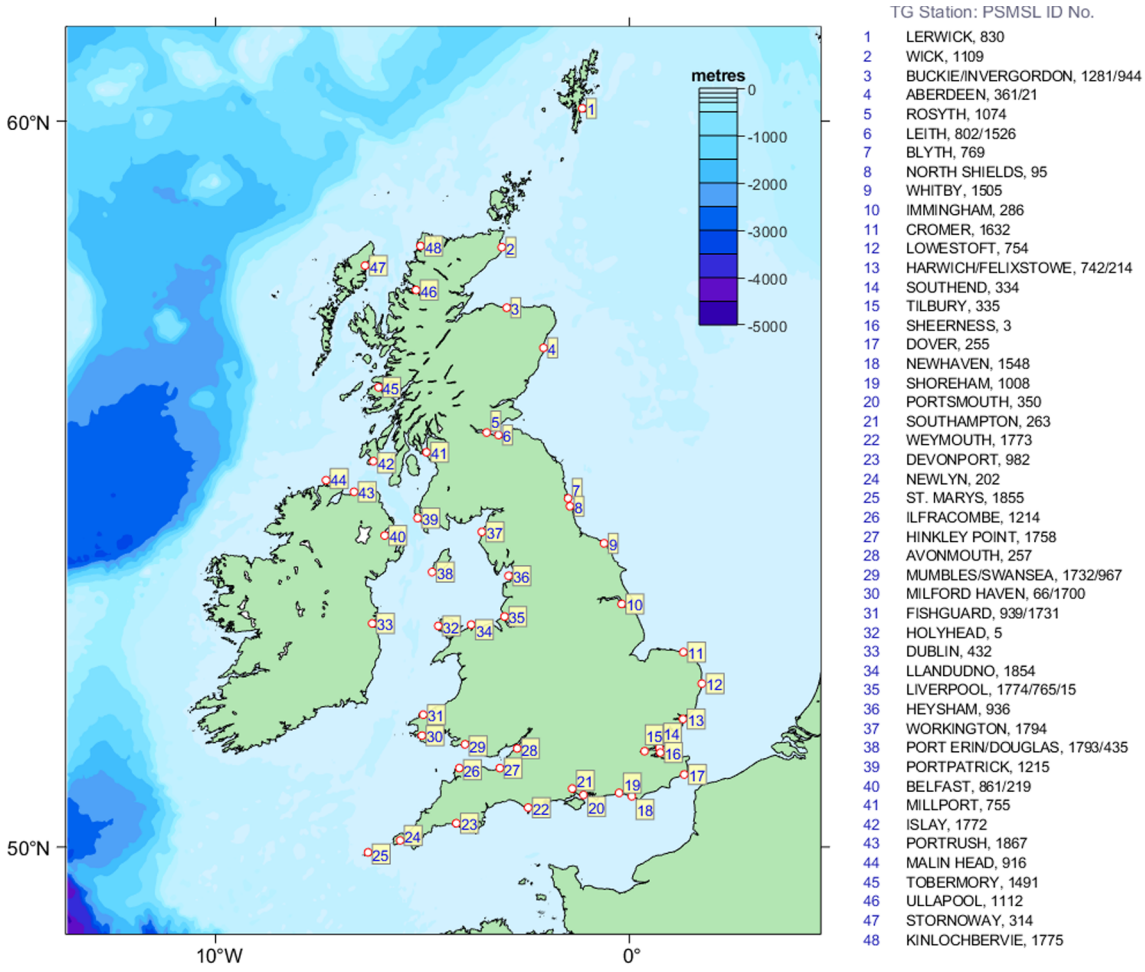

Fig. 1. Tide gauge stations around the British Isles with more than 20 years of data, indexed starting at the northernmost station in Shetland, then clockwise around the coastline, with station name and PSMSL station number (or numbers if composite). Sites will use the index numbers (in parentheses) throughout this paper to ease reference.

Dangendorf et al. 2014; Haigh et al., 2009; Haigh et al., 2014; Frederikse et al., 2016a; Frederikse and Gerkema, 2018). This paper can be viewed as part of this ongoing process.

The Permanent Service for Mean Sea Level (PSMSL) is the main repository for global tide gauge data (Holgate et al., 2013). The 'Metric' MSL dataset contains monthly means of the original data for each site and is usually referenced to the tide gauge zero (TGZ) that was used at the time of recording (further background is given in Supplement 1). The Metric data therefore normally retains all the original (often large) TGZ changes, reflecting events such as gauge relocation or replacement, or redefinition of local Admiralty Chart Datum (ACD) (Aarup et al., 2006). The Revised Local Reference (RLR) dataset represents quality-controlled monthly mean data where records of these changes allow correction (as far as possible) to a consistent local land-based vertical reference point. Whilst the records have been subject to review, comparison and quality control over many decades (Graff and Karunaratne, 1980; Woodworth, 1991), a portion of the Metric data has not been reduced to RLR as the elevation differences between the TGZ and local bench marks were unknown or uncertain. In order to maximise the amount of useable data we initially carried out a data archaeology exercise (see Section 3) which allowed the recovery of new (as well as verification of existing) information, increasing the number of sites around the British Isles where RLR type offsets can be applied. The degree of this data extension is summarised in Fig. S5 in supplement 1. In all, the PSMSL holds monthly MSL data of varying record length and quality for around 100 sites around the British Isles. By including the newly extended and composite records, we increase the number of sites which have 20 or more years of data over the period from the late 1950 s to the end of 2018 from 34 to 48.

The tide gauge measurements around the coast of the British Isles are affected by a range of different physical processes. These include: responses to local atmospheric pressure (Doodson, 1924; Ponte, 2006); wind stress (Thompson 1980; 1981) including tide and storm surges (Frederikse et al., 2016a; Frederikse and Gerkema, 2018); a response to more distant ocean variability (Wakelin et al., 2003; Calafat et al., 2012; Frederikse et al., 2016b; Volkov et al., 2019) which modulates and includes global mean sea level changes; local vertical land motion (VLM) (Wöppelmann and Marcos, 2016) due to present day processes (such as localised subsidence due to groundwater extraction, or potentially for North East England, coal mining) (Rossiter and Gray, 1972); and both land and gravitational responses to past glaciations, known as Glacial Isostatic Adjustment (GIA) (Bradley et al., 2011). Of these, the meteorological response and GIA response are expected to vary substantially, while the response to more distant ocean variability is expected to be more consistent from gauge to gauge. In Sections 4.3 and 5.3 we exploit this understanding.

Section 2 describes the data sources, and Section 3 the data archaeology (more detail on the kinds of data sources and details of tide gauge datum determination are given in supplements 1,2 and 3). In Sections 4 and 5 we work through the data improvements, using two example tide gauge sites in Section 4, and then the entire dataset in Section 5. These improvements take the following form:

- Step 1 (Sections 4.1 and 5.1): Add levelling information to Metric

and newly found data to produce the extended, RLR-quality Metric Extended Reduced dataset, with no further datum correction at this stage.
- Step 2 (Sections 4.2 and 5.2): Perform "buddy checking" against nearby tide gauges, where possible, to demonstrate that previously undetected datum steps are visible, and make an estimate of their times.
- Step 3 (Sections 4.3 and 5.3): Minimise variability to make datum steps more visible. This is done by (a) subtracting variability due to modelled GIA and the response to local meteorology from a barotropic ocean model, to make the time series at different sites more strongly correlated, (b) creating a detrended Initial Common Mode, as an average of all tide gauge time series from a), each quadratically detrended. (c) subtracting this Initial Common Mode from each detrended tide gauge, to make a time series in which datum steps are more clearly detectable.
- Step 4 (Sections 4.4 and 5.4): Identify "events", defined as times at which steps are likely to occur due to tide gauge changes (each event must be confirmed by a coincidence of an observed step and, usually, the time of a documented tide gauge change or, occasionally, a step identified from buddy checking with two other tide gauge records).
- Step 5 (Sections 4.4 and 5.5): Apply vertical offsets to segments of records between events. These offsets are in most cases derived from independent datum information. Where this is not available ("free-floating" segments), steps are estimated by minimising the difference from the quadratic trend derived from the constrained data.

Section 4.6 validates the adjustment procedure for "free-floating" segments, by comparing different methods, and the end of Section 5 describes the changes which have been made by all these datum corrections.

Section 6.1 discusses the variability in the resulting improved, detrended time series, and Section 6.2 shows that, when the trends are retained, the new data now shows much more consistent linear trends. In Section 6.3 we introduce the Final Common Mode – an average of all tide gauge sites after removing variability and datum steps – and show that the scatter of trends relative to this average is substantially reduced. Section 6.4 shows that the final data show much better agreement on sea level accelerations, that the Final Common Mode is robust, and that its interannual to decadal variability comes from a mode common to the eastern boundary of much of the North Atlantic.

Finally in Section 7 we summarise the results and draw conclusions.

2. Data and sources

In this paper we use various observational and model datasets to account for observed variability in the tide gauge time series. The analysis period of Jan. 1958 to Dec. 2018 is limited by the availability of the CS3X tide and surge model (latest version of the Extended Area Continental Shelf tide and surge model, see description below, and https://www.ntslf.org/storm-surges/storm-surge-model). The seasonal cycle was removed from each time series by simultaneous least squares fitting of annual and semi-annual sinusoids (application of this method leads to data described as "deseasonalised" below).

Monthly MSL data (Metric and RLR data sets) for waters around the British Isles (Fig. 1) was obtained from the PSMSL (Holgate et al., 2013), https://www.psmsl.org/data/ augmented by other sources. These included the Irish Office of Public Works (http://waterlevel.ie/hydro-data/stations/40060/station.html) for updated data from Malin Head; the Channel Coastal Observatory reports (https://www.channelcoast.org/reports/); data from the British Oceanographic Data Centre (BODC); from recently published research (Haigh et al., 2009); and small amounts of additional unpublished "new" data recovered from the National Oceanography Centre (NOC) archives. The data archaeology exercise covered all periods of tide gauge observations, but in most of the analysis here we use data from the years Jan. 1958 to Dec. 2018 inclusive.

The annual MSL data from a global mean sea level reconstruction (Church and White, 2011, updated to 2013) was downloaded from: https://www.cmar.csiro.au/sealevel/sl_data_cmar.html. We also downloaded the hybrid reconstruction of monthly global MSL estimates from Dangendorf et al. (2019) at https://doi.org//10.1038/s41558-019-0531-8. These are already GIA corrected and are used for comparison and global context.

Gridded satellite altimetry absolute dynamic topography at 1/4° resolution from Segment-Sol multimissions d'ALTimétrie, Orbitographie et localisation précise/Data Unification and Altimeter Combination System (SSALTO/DUACS) was downloaded from Copernicus Marine Environment Monitoring System at http://marine.copernicus.eu/. This product has already been adjusted for the inverse barometer effect (Carrère et al., 2016). Monthly mean equivalent sea surface height (SSH) time series were extracted from grid points near each tide gauge location. These represent local MSL relative to a geocentric reference frame, but the data is only available from 1993 onwards. This data was used for comparison with tide gauge data over the satellite period.

Sea level variability due to local meteorological influence is estimated using CS3X, a variant of the UK's main operational tide-surge forecast model (e.g. Flather and Heaps, 1975; Flather, 2000; Flowerdew et al., 2010). Modelled monthly mean sea level was extracted from hourly time series of sea level variability due to tide and surge at each tide gauge site, simulated from Jan. 1958 to Dec. 2018. The domain spans 20°W to 13°E, 40°N to 63°N, with a resolution of 1/9° latitude by 1/6° longitude (approx. 12 km, see https://noc.ac.uk/files/documents/business/model-info-CS3X.pdf). The open boundaries are forced with an assumed constant sea level plus local inverse barometer response to atmospheric pressure, and tidal constituents from a tidal analysis of an outer CS3X-like model of the northeast Atlantic (Flather, 1981). The atmospheric forcing is 6-hourly wind and sea-level pressure from ERA-40 (Uppala et al., 2005) over the reanalysis period (1 Jan. 1958 to 31 Aug. 2002) and from Met Office operational hindcasts from the Met Office operational atmospheric model (Unified Model) thereafter.

We use a GIA correction (Emery and Aubrey, 1985; Peltier and Tushingham, 1989; Whitehouse, 2018) given by the Peltier ICE-6G_C (VM5a) model (Peltier et al., 2015; Argus et al., 2014), available from http://www.atmosp.physics.utoronto.ca/~peltier/data.php. The correction we apply includes gravitational effects as well as vertical land movement, removing the secular component of RSL (relative sea level) that results from GIA (Tamisiea, 2011). Other GIA models are available for the UK, (as are CGPS (Continuous Global Positioning System) based estimates of recent vertical land motion). Other models we looked at were similarly effective in reducing the scatter in these trends.

3. Summary of data archaeology

A data archaeology exercise was carried out using historical documents archived at the NOC (Liverpool), UK Hydrographic Office (UKHO) archives (Taunton) and older editions of large-scale Ordnance Survey (OS) maps (online). These comprised OS levelling records, tide gauge calibration records, annual Admiralty Tide Tables, Institute of Oceanographic Sciences (IOS) and National Tidal and Sea Level Facility (NTSLF) reports, paper records of tide gauge history (e.g. Tide Gauge Inspectorate (TGI) reports) and large amounts of correspondence between the UKHO (and many others, e.g. individual port authorities) and the PSMSL. This resulted in additional information being recovered for each tide gauge site, such as older local bench mark elevations, semi-annual or annual tide gauge zero check sheets, Ordnance Survey tide gauge zero levelling history (summarised in OS-319 sheets, see supplementary material 2), and elevation changes to the local port or chart datum.

The recovery of additional datum connections and bench mark elevations allowed extension or creation of time series referenced to a

consistent site datum (RLR-style) at several locations (e.g. Stornoway, Ullapool, Newhaven, Shoreham, Blyth) and new composite series to be created (e.g. Swansea and Mumbles, Invergordon and Buckie, Harwich and Felixstowe, and the two records from Leith) similar to the process used previously for Aberdeen and Liverpool (Woodworth et al., 2009). In this case the use of Ordnance Datum Newlyn (ODN), or Local Ordnance Datum on island sites aids the comparison of elevations of older and modern benchmarks, and also has the effect of making the absolute levels more comparable between tide gauges, especially locally. We refer to the data after correction to a common reference datum as "reduced" data.

Any average offset adjustments required due to sections of data being Mean Tide Level (MTL) rather than MSL were also made (Suthons, 1937; Hogarth, 2014; Woodworth, 2017). These adjustments vary from station to station and can be centimetre scale. This reanalysed MSL data was checked against the PSMSL RLR time series. Any offset between the reanalysed Metric data and the RLR series should be constant and equal to the difference between the RLR reference elevation and the mapping datum (ODN) given in the PSMSL RLR diagrams. A small number of anomalies were investigated and resolved or explained (e.g. Portsmouth and Devonport).

A tide gauge 'event' file was created for each site by digitising all recorded physical changes which could potentially affect the tide gauge zero. These were extracted from OS 319 sheets (these are detailed in supplements 1 and 2), TGI records and correspondence files. This information has been summarised in a MATLAB® script containing change event dates and brief descriptions for each site, indexed by PSMSL site number (see supplementary material 3).

The six-monthly or annual measurements of tide gauge zero elevation changes relative to the tide gauge bench marks were also recovered and digitised for the 35 sites where OS 319 sheets were available, as were the equivalent recorded levelling measurements available for Malin Head. 'Calibration' files were created for each site, containing a list of observation dates and measured differences between the measured TGZ and assumed TGZ elevations.

4. Method, case studies: data processing steps

4.1. Data extension

The PSMSL RLR monthly MSL record for Stornoway (site 46, see Fig. 1) starts in 1977, but there is also a year of Metric data from Nov. 1928, and an almost continuous record from January 1957. The data archaeology exercise allowed recovery of the relative TGZ and bench mark elevations from these additional periods, resolving the large datum steps and thus extending the time over which a consistent datum could be applied by an additional 252 station months, adding another 50% to the existing RLR record (Fig. 2). This extension process was repeated where possible for each site around the British Isles, giving a new extended monthly MSL dataset (here reduced to ODN), which we call the "Metric extended reduced" (MER) dataset. This dataset was then deseasonalised and adjusted for GIA using the Peltier ICE-6G_C (VM5a) model (Peltier et al., 2015).

The Metric record from Immingham (10) over the Oct. 1959 to 2018 period also has a large recorded datum difference of over 7 m after the end of 1985. This has already been accounted for in the PSMSL RLR record. The site records of tide gauge zero and local bench mark elevations give the relative datum offsets needed to reduce the Metric data to ODN and these validate the elevation values in the site RLR diagram from the PSMSL. However the GIA-compensated SLR trend derived from the Immingham time series is less than 1 mm yr^{-1}, whereas the neighbouring gauges with long and relatively complete time series at North Shields (8) and Lowestoft (12) (approx. 173 km north and 182 km south of Immingham respectively) have trends of over 2 mm yr^{-1} over the same period. The anomalously low trend at Immingham has been previously attributed to known density changes in the river Humber run-off (Woodworth et al., 2009; Haigh et al., 2009).

4.2. Buddy checking

The time series from Immingham was then 'buddy checked' (Rude, 1926; Woodworth, 1991) against similarly adjusted MSL records from the two sites above. Fig. 3 shows plots of the differences (Immingham minus North Shields and Lowestoft monthly MSL respectively). Taking differences of records from nearby sites effectively removes any additional coherent "common mode" variability (for nearby sites this will include both local and far field effects), revealing several clear steps after year 2000, and two more ambiguous ones before that date. Various techniques were tried to automatically detect and quantify the steps seen. Using the maximum likelihood changepoint detection function implemented in MATLAB® (Lavielle, 2005; Eckley et al., 2011; Killick et al., 2012) on each difference plot gives an estimate of the most probable change points in mean difference. If the time and magnitude of any detected changes are the same in both comparisons (within some defined tolerance), then the change probably originates from the shared time series, i.e. Immingham (see also Caussinus and Mestre, 2004 for other examples of this methodology). These coincident detected change points are shown as green dashed lines.

However independent information is needed to confirm the timing of the steps, and the "buddy" checking relies on having good quality and near complete data from neighbouring sites. This is not always available, so various other methods were explored to reduce the variability in the MSL records, including the use of barotropic models and a common mode (Woodworth et al., 1999).

4.3. Adjusting for local and far field sea level variability

The top (blue) trace of Fig. 4 shows the deseasonalised monthly MSL data for our case study site of Immingham. The sea level response to local meteorological effects (inverse barometer and wind stress) can be accounted for by subtracting the mean monthly CS3X modelled sea level, which is derived purely from a reanalysis of atmospheric pressure and wind observations.

The middle (red) trace of Fig. 4 shows the result. The meteorologically induced high frequency variability is greatly reduced, but lower frequency components remain largely unaffected. This is expected as the tide and surge model itself contains little interannual to multidecadal variability. Comparing with similarly processed data from other sites around the British Isles confirmed that these low frequency fluctuations appear coherent. Consistent with the buddy checking results, removing a "common mode" which contains these low frequency signals (Larsen et al., 2003) results in a further reduction in variability, as shown by the residual in the bottom (purple) trace of Fig. 4. This Initial Common Mode (ICM) is here defined as the average detrended (first and second order) MSL for all stations, with individual tide and surge model data removed. Note that this ICM is used purely to reduce variability and aid in detection of steps. We will later produce a Final Common Mode (FCM) which retains all trends, and where any potential bias due to averaging different record lengths is minimised (see supplementary material 1) and tested by using various combinations of records. It is thought that this "common mode" signal will reflect broader scale ocean variability originating from beyond the local shelf region (Chafik et al., 2019). Unlike buddy checking, this two-step process effectively separates far field ocean effects from local meteorological effects. We find that combining CS3X with a common mode best reduces the natural variability seen at most tide gauges.

Referring to Fig. 4, as the variability is progressively reduced, a number of clear datum steps emerge, e.g. in 2000 and around 2012. In addition, comparing the adjusted time series from neighbouring sites reveals apparent trend similarities in sections unaffected by these steps. This suggests that much of the difference in SLR trend between

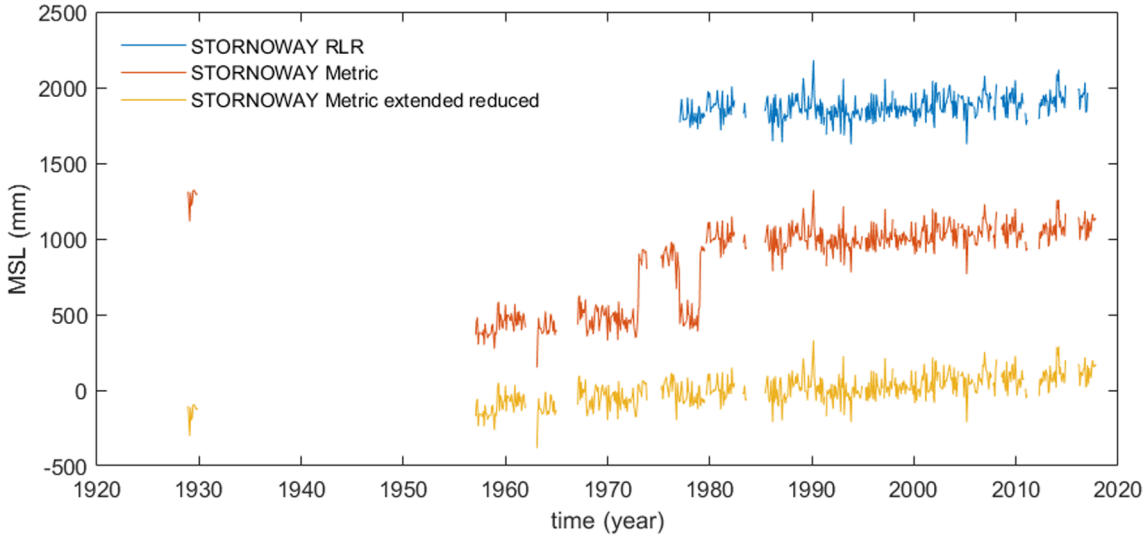

Fig. 2. Deseasonalised monthly MSL for Stornoway; PSMSL RLR, PSMSL Metric, and Metric extended reduced data using recovered datum connection information. Each time series is offset vertically for visualisation.

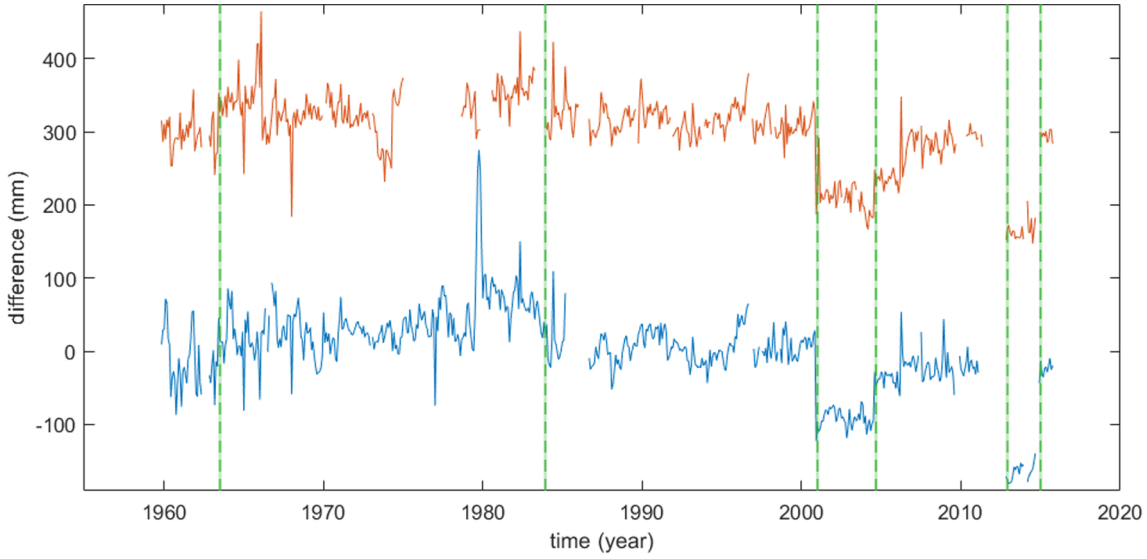

Fig. 3. Difference plots of reference MSL minus model series from nearby sites, with detected change points. Red: Immingham minus North Shields (offset 300 mm for visualisation). Blue: Immingham minus Lowestoft. Change points which are common to both difference plots are dashed green. (For interpretation of the references to colour in this figure legend, the reader is referred to the web version of this article.)

Immingham and nearby gauges can be explained by the presence of these datum shifts (see also Becker et al., 2009 for trend differences due to datum shifts in records from the coast of Holland). Thus, the subtraction of tide and surge model plus common mode data allows for similar discrimination of steps to that found by high quality buddy checking, but we still require more information to help interpret the steps that are seen.

4.4. Identifying and quantifying datum steps

Fig. 5 shows the deseasonalised and detrended monthly MSL data for Immingham, with modelled storm surge data and the initial common mode subtracted (blue, see supplementary material 1 for detrending method used at this stage).

Initial attempts were made to quantify the step timing and size using a variety of change point detection methods (Beaulieu et al., 2012). Using the Mann-Whitney test and basic differential methods (Trauth et al., 2018) showed false detect issues typical of the 'change point detection problem' (Gallagher et al., 2013). A more flexible and robust method used the MATLAB® maximum likelihood change point function. For Immingham, nine changepoints are detected, as shown by the orange line in Fig. 5.

The data archaeology exercise allowed a record of all physical change events which could potentially affect the datum to be created for each site (supplementary 3). For Immingham these are shown as grey vertical lines in Fig. 5. Importantly, many of these events are associated either with breaks in the time series, or apparent datum shifts. Many of the detected changepoints (orange) are seen to coincide with recorded events (grey), as well as the independent results of the buddy checking from the two other sites illustrated previously. The buddy checking process also gives some additional changepoint times which were unrecorded (e.g. late 1983). These are shown as green vertical lines in Fig. 5. We find after reviewing all sites that the recorded events augmented with the buddy checking results capture the times of almost all visible datum shifts, and the majority of changes detected using the maximum likelihood function. We also investigated a number of high resolution records (15 min sampling) which confirmed that steps were usually associated with breaks in data continuity, implying a physical change. Thus, these recorded events, and those buddy-checking steps

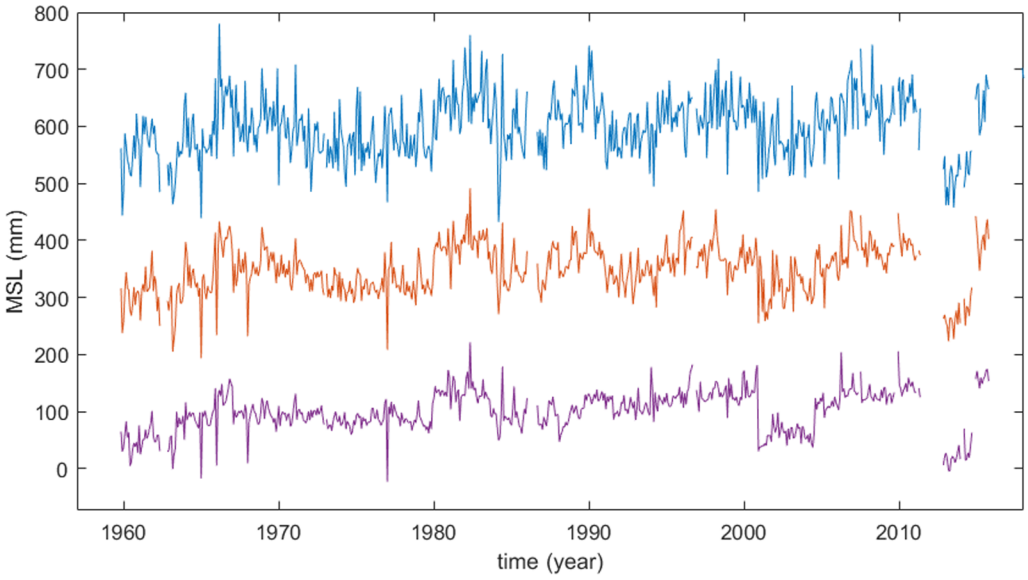

Fig. 4. Plot showing progressive reduction of variability in monthly MSL time series from top, blue: deseasonalised MSL data with initial datum adjustments. Red: deseasonalised data adjusted for CS3X tide and surge model. Purple: Adjusted using CS3X and common mode. Each time series is offset by 200 mm to aid visualisation. (For interpretation of the references to colour in this figure legend, the reader is referred to the web version of this article.)

which are confirmed by the model-based jump detection, give us an objective set of break points at which we should seek information on datum changes (Li and Lund, 2015). We only consider detected jumps which are confirmed by at least one other source of information. These are then referred to below as "events".

4.5. Adjusting for datum steps

For Immingham, semi-annual or annual tide gauge zero reference (Van de Casteele tests, Lennon, 1968) and repeat levelling measurements by the OS are available from the early 1960 s to the mid-1980 s (OS 319 sheets, see supplementary material 1 and 2 for explanation and examples). These record some of the known instrumentation changes. Normally a time average of these levelled calibrations was used by the UKHO and PSMSL to define the TGZ. The discrete 'calibration file' offset values for this site are plotted as red circles in Fig. 5. These represent the differences between the accepted TGZ value used by the PSMSL (usually the UKHO "Admiralty Chart Datum" based on some fixed definition of observed Low Water level) and the measured TGZ elevations. As has been demonstrated previously in the case of Portsmouth (Webber and Walden, 1981; Walden, 1982; Haigh et al., 2009), additional information is available which has not been fully exploited. In this case, datum level changes around 1963 and 1980 appear to be recorded, and evidence for a downward step in late 1983 from the buddy checking is validated by a measured elevation change.

We investigated several ways to use the sparse calibration data to adjust the monthly records (e.g. using interpolation between the calibration dates), but after reviewing the results from all sites we concluded that the most robust method was to use an average of the calibrations over each period between 'event' times (i.e. the levelling information is used, but averaged over segments of data between our confirmed change points). Applying these offsets (Table 1) corrects the section of relatively high data between the end of 1979 and 1983 so that it is no longer discernible (or detectable, Fig. 6). By contrast, the short upwards excursion in 1966 is unaffected. This latter anomaly is also visible in nearby tide gauge records, so is likely to represent real

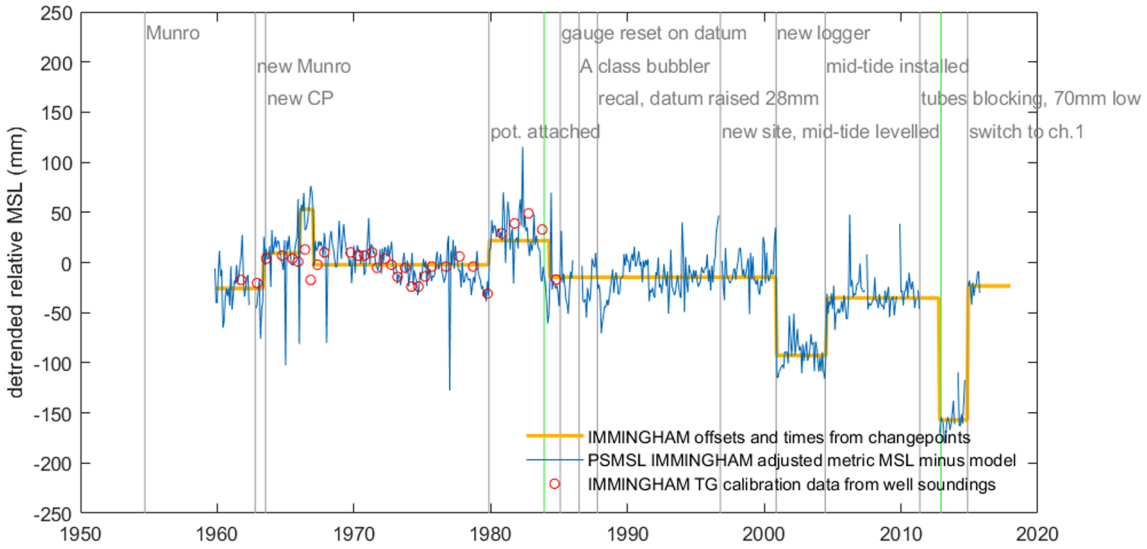

Fig. 5. Plot of deseasonalised detrended monthly MSL minus surge model and common mode for Immingham. Results of auto change point detection and segment mean values are shown in orange. Recorded physical changes at the site are shown as vertical grey lines with the labels running in groups of four stepping sequentially downwards and to the right. Any additional changes common to two independent buddy checks are shown as green vertical lines. TGZ differences from recorded datum (OS levelling) are shown as red circles. (For interpretation of the references to colour in this figure legend, the reader is referred to the web version of this article.)

Table 1
Top: Offsets (mm) for Immingham derived from calibration up to 1984, and levelling (bold) combined with regression after 2001. This is the method used in this analysis. Next two rows, offsets derived from differences between data and modelled sea level for 36 months before and after event. Next, offset and time estimates from changepoint detect process. Bottom three rows, offsets and mean time of detected changes for buddy checks for three long and relatively complete records.

Year: Event	1963.62	1979.96	1983.96	2000.96	2004.46	2012.96	2014.96
Using cal. and regression	24	48	−55	−79	55	−123	133
Offsets from Surge Model				−79	48	−157	133
Year: changepoint detect	1963.46		1983.71	2000.96	2004.62	2012.87	2014.96
Offsets: changepoint detect	35		−51	−78	60	−119	136
Year: Buddy check	1963.54		1983.96	2001.04	2004.71	2012.96	2014.96
Buddy check North Shields	46		−39	−94	49	−129	130
Buddy check Lowestoft	42	59	−55	−96	62	−143	139
Buddy check Newlyn	42	49	−51	−100	57	−133	105

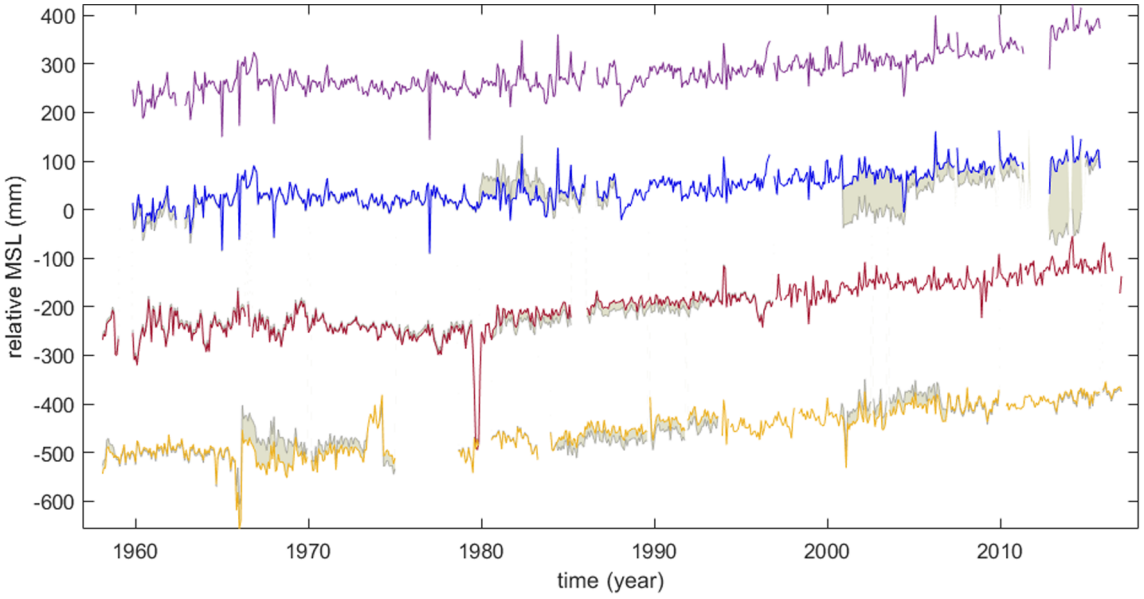

Fig. 6. Top, purple: adjusted Metric MSL data for Immingham, result of subtracting the individually estimated offsets derived from mean difference values for up to three years either side of each change. Blue: adjusted Metric MSL data for Immingham, result of alternative datum step adjustment using calibration data up to 1984 and segment-based regression thereafter. Grey shading shows data before adjustment and magnitude of correction. Red and orange show North Shields and Lowestoft respectively, treated in the same way with the relatively small datum adjustments for these sites again in grey. The negative spike in the Lowestoft record just before 1980 is normally flagged as an error and removed in the RLR record. Each time series is offset 250 mm for visualisation. (For interpretation of the references to colour in this figure legend, the reader is referred to the web version of this article.)

local sea level variation (which might otherwise be removed by a naïve change point detection process).

Several datum shifts are also visible after a bubbler gauge was installed in July 1986 by which time TGZ levelling checks had become intermittent. Nonetheless, some segments, in this case those up to the year 2000, do have levelling data associated with them (note the levelling which is recorded along with the installation of a new site in 1996). As with the regular calibration period, these segments are also 'fixed' with reference to ODN using the average of the levelling and calibration data over those segments.

Other segments (in this case all those after the installation of a new logger in 2000) are considered here as "free floating". The magnitude of corrective offsets for these "free floating" segments can be estimated by a number of methods (Table 1): by using mean differences for short sections before and after each change event (purple curve in Fig. 6); or by buddy check comparisons; or by allowing each segment of data between known change events over the entire extent of the record to be offset and fitted to a best fit (least squares regressed) linear trend and second order function (blue curve in Fig. 6). The second order term was included as it best explained the largest proportion of the low order non-linearity apparent in the majority of longer series, and retaining this signal in each processed series is of interest (a similar rationale is behind the ICM being quadratically detrended).

4.6. Validation

A comparison of these independently derived step offset values (Table 1) can give some measure of confidence in each estimate. For example for December 2014 the change detect method gives an estimated positive step of 136 mm, the buddy check comparisons give 130 mm and 139 mm respectively, whilst the surge model difference and regression both give 133 mm. An additional check with the high quality record (Bradshaw et al., 2016) from more distant Newlyn gives 105 mm. The comparisons for the change point detect and buddy check also show some differences in timing of the steps as the unconstrained estimate of change time also has uncertainties. Comparisons can also be made for the period from 1993 onward with gridded satellite altimetry data, provided that variability due to meteorological effects is similarly minimised. For Immingham the adjusted TG minus local altimeter MSL trend is 0.025 mm yr^{-1}, whereas the unadjusted TG minus altimeter MSL trend is −3.7 mm yr^{-1}. The adjustment process will thus greatly impact estimates of VLM based on TG minus altimetry data, where the effect of datum shifts in the TG data on the residual trends is compounded by the relatively short altimetry period.

The offset adjustment values used for this paper are the calibration results (For Immingham, table 1, top row) over the period these are available (approximately the first half of the record in this case), and

the levelling constrained regression results over the rest of the record. All series have seasonal, GIA, surge model and common mode adjustments. The time series after step removal more closely resembles those of other sites on the East Coast which appear to be less affected by datum shifts, as shown in the comparison with Lowestoft and North Shields in Fig. 6.

While this process is useful for unifying the time series, it is important to bear in mind the difference between those segments of data which have been fixed by levelling (offsets in bold for Table 1), and those which have been adjusted based on some kind of reasonable expectation of short term consistency (smoothness) of the difference between measured and modelled data. It is also important to contrast the differences between this "event" constrained approach and unconstrained approaches based on changepoint detection. Initial attempts at blind step detection showed this naïve approach will inevitably remove low frequency components of natural variability as well as steps if the magnitudes of the low frequency fluctuations are similar to or greater than that of the datum steps. We show later that this step adjustment is less of a problem when the step times are limited to confirmed events.

This section has illustrated the approach in the context of two particular tide gauges. In the next section we summarise the various stages as applied across the wider range of gauges from around the British Isles. We will show later that this results in improved consistency between long term trends measured at these sites.

5. Application to all tide gauges around the British Isles

5.1. Data Extension

The process described for Immingham was automated and repeated for all sites. The first stage is to independently replicate the Metric to RLR conversion performed by the PSMSL, but using the extended information and metadata provided by the data archaeology initiative. The results of this are shown in Fig. 7 compared with RLR data. Newly reduced data comprise 9542 station-months in addition to the 22,485 station-months already in the RLR dataset for the sites studied, a 42% increase in available data, including some data not in the PSMSL Metric dataset (e.g. from Southampton and Belfast). A graphical overview of the extent of the various MSL data used is also given in Fig S5 in supplement 1. Any large "spikes" (see Fig. 5) which are normally flagged in RLR data were identified using a modified version of the function described in Feuerstein et al. (2009), where the spike data values were removed rather than replaced with interpolated values. Tower Pier (a station on the river Thames in the Greater London area) was rejected at this stage due to high variability associated with run-off causing river level fluctuations which were not captured in the tide and surge model, giving 48 stations (Fig. 1). For each site, a list of recorded instrumentation changes was also created from the data archaeology exercise.

5.2. Buddy checking

We now perform buddy checking. This helps initially to identify some likely datum shifts. Where two buddy stations show a coincident datum change of similar size, the majority of these are also found to coincide with known instrumentation changes at the common site. A small number of coincident buddy check steps are found not to be associated with known changes, but most likely reflect an unrecorded event. For these, the timing is derived using results from the change point detection averaged for both buddy check difference series. These times are then used to augment the recorded event times in order to objectively capture all independently detectable step changes.

5.3. Adjusting for local and far field variability

Following this, the local modelled GIA trend and detrended modelled monthly mean tide and surge response plus common mode were subtracted from the tide gauge data for each site. The maximum likelihood change point analysis was applied to again help identify potential steps. As with Immingham, it is clear that datum steps exist in a number of records, and that these are responsible for significant long-term differences in trends between gauges. Those steps which had independent confirmation, mostly from documented instrumentation changes but in some cases from buddy checking, were used to create event files for each site, and these event times were used to divide the data into segments for adjustment.

5.4. Quantifying datum steps

The tide gauge levelling and calibration results from OS-319 sheets (supplement material 2) were then digitised for the 36 sites at which they were available. The equivalent levelling information was also digitised for Malin Head on the Irish Coast. Records from some of the sites where calibration data is available (e.g. Harwich and Felixstowe) have been merged into longer composite MSL records. A small number of sites have calibration data but no available MSL data. This reduces the number of sites where systematic calibration results can be used to 33 (Fig. 8), and of these, only 28 have more than 20 years of data (centre panel Fig. 9). The measured TGZ values were double checked against the original Van de Casteele calibration test results (see Lennon (1968)) and bench mark information (see supplement material 1).

5.5. Adjusting for datum steps

The levelling results were then applied to those site-segments for which they were available (generally covering the period from the early 1960 s to the mid-1980 s), and then "free floating" segments were adjusted by least squares fitting a linear and quadratic trend plus offsets to each series of the entire dataset, with offset adjustments only permitted on the "free floating" segments (Fig. 9). As with Immingham, not all post 1980 s segments are "free floating", for example many segments are "fixed" using levelling information related to the installation and calibration of mid-tide sensors (Woodworth et al., 1996).

In summary, each residual tide gauge time series (with surge model and ICM subtracted off) was cut into segments bounded by fixed "event" times. These events are defined as times of documented equipment changes, with occasional additions where dual buddy checking gives additional times. These were then checked against the results of an automatic step-detection process. Levelling information was used to fix the datum in all segments for which it was available (coloured segments in the right hand panel of Fig. 9). Other "free floating" segments were then offset so as to minimise the difference from a quadratic fit to the data which are not "free floating", and the offset values were independently buddy checked. The quadratic trend of each time series is therefore determined only by the levelled segments. As a further independent check, the sections of time series from 1993 to 2017 were then compared with the 0.25°gridded altimeter monthly mean MSL data, using both the nearest grid cell and an average of nearest grid cells to each tide gauge. The overall processing steps are shown graphically in Fig. S6 supplement 1.

The final step offset values (the signals to be subtracted from each record to correct for datum jumps) referenced to the nominal TGZ for each site can in some cases exceed 100 mm (Fig. 10a). Any impact of the average datum correction signal (Fig. 10b) on the existing mean SLR trend for the British Isles will be small as there is little correlation of data step times or magnitudes between sites, and the resultant pseudo-noise averaged offset signal has little bias (here, the small -0.1 mm yr^{-1} negative trend introduced by datum steps means that, after correction, the adjusted trend is increased by $+$ 0.1 mm yr^{-1}). Similarly the small acceleration term in the error signal will reduce the acceleration slightly in the final averaged result (see Table 2).

5.6. Trend analysis

New SLR trends and formal uncertainties were then derived. We accounted for coloured noise in the trend fitting process by using the

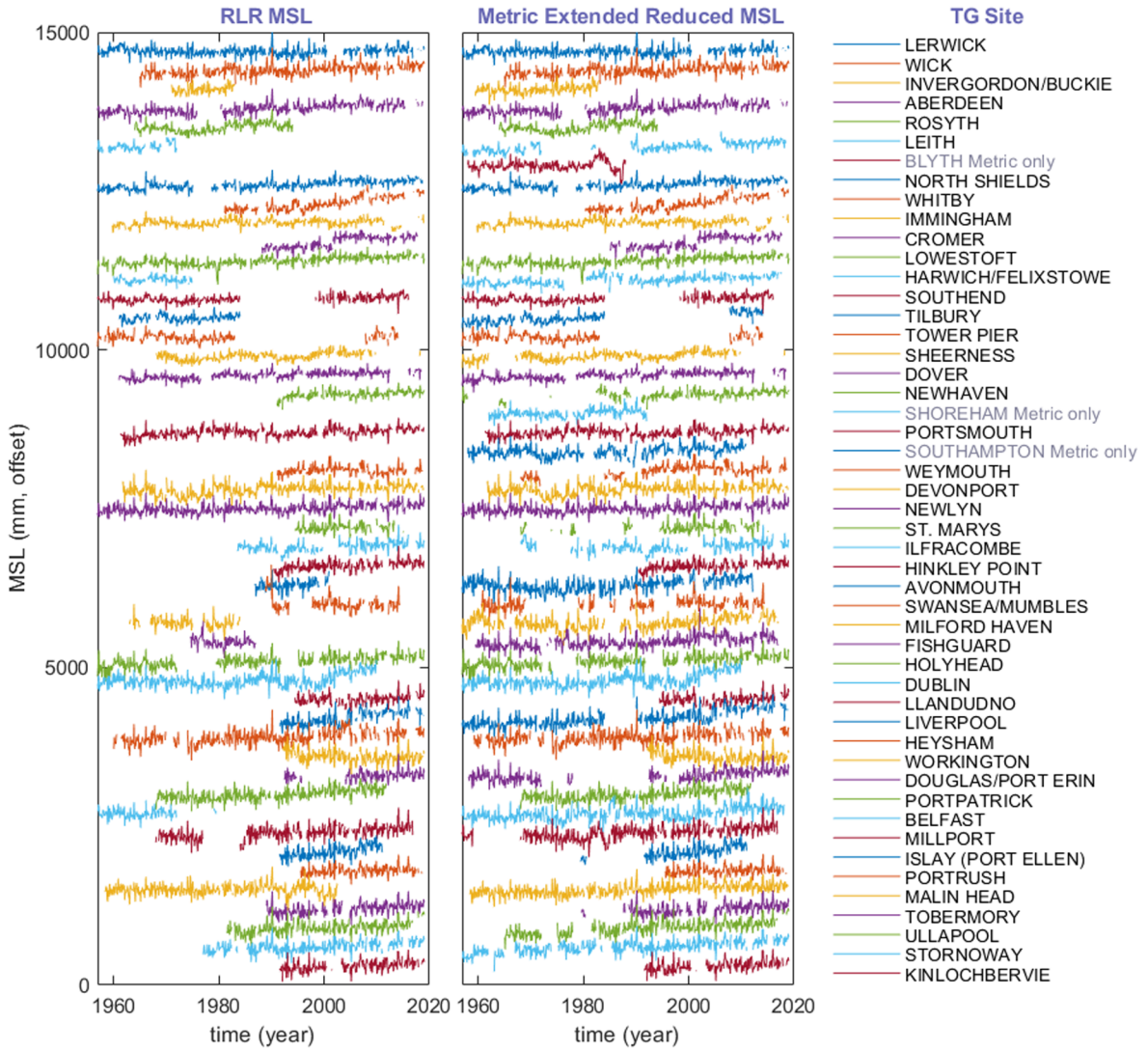

Fig. 7. RLR monthly MSL from PSMSL compared with Metric extended reduced MSL Jan. 1958 to Dec. 2018, deseasonalised and adjusted for GIA (49 sites with a span of more than 20 years of extended data shown here). Each series offset by 300 mm for visualisation. Data steps are not immediately apparent at this stage.

CATS (Create and Analyse Time Series, Williams, 2008) software on each time series (Williams, 2008; Bos et al., 2013). The effect of the datum step adjustments at individual stations can be profound, in some cases even reversing the SLR trend, as at Workington (37) (Fig. 11). Here uncorrected negative steps are apparent in the record, two of which have been previously noted (Hames et al., 2004). Initial tape measurements were made by divers from underwater pressure ports to a fixed point above water during installation of the pressure-based system in 1992, and later datum "corrections" are recorded in September 2002 and June 2004, but only the latter involved levelling to OS bench marks. A naïve interpretation of the unadjusted data would conclude that sea level was falling at this site. The reconstructed data with offsets adjusted assuming the final segment only is fixed has a trend which closely agrees with that from other sites.

The trends for the majority of sites derived in this systematic manner are now more comparable to those derived from the small number of RLR sites typically selected and judged to be of high quality (this has been partly a subjective expert assessment to date) (Woodworth et al., 1999). A few sites appeared not to fit the general pattern, these were found to be associated with factors such as jetty subsidence (e.g. Islay (41)), although for some sites anomalous changes in apparent relative sea level previously attributed to subsidence could be re-assessed in the light of the detected datum shifts.

5.7. Troublesome cases

A small number of the tide gauge time series remain problematic. For example gauge malfunctions are recorded at Malin Head between 1998 and 2003, and these correspond to lowered MSL anomalies in the data (Fig. 12, blue). These sections of data are probably irredeemable and should be flagged and removed from any trend analysis (as some of them already are in the PSMSL RLR data), but this leaves considerable gaps. A more continuous representation of local MSL can be created by replacing the problematic section using data from nearby working gauges. As with any composite series, this depends on land motion and datums at the original and buddy check site being known. If the infill section overlaps unaffected data and differences are within acceptable error bounds, this gives confidence that this is a reasonable processing step. For Malin Head (44), the bubbler gauge record from Portrush (43) can be used (Fig. 12, red) which would otherwise be too short to contribute to the site by site multi-decadal analysis (as it starts in 1995). This also provides evidence for the small datum shift detected in the Malin Head data at the beginning of 2013 (Note that the Malin Head data from 2003 onwards is not yet in the PSMSL, but is available elsewhere, see data section previously)

For sites such as Southampton (21), Dublin (33) and Belfast (40), sections of relatively high variability indicate low quality data and/

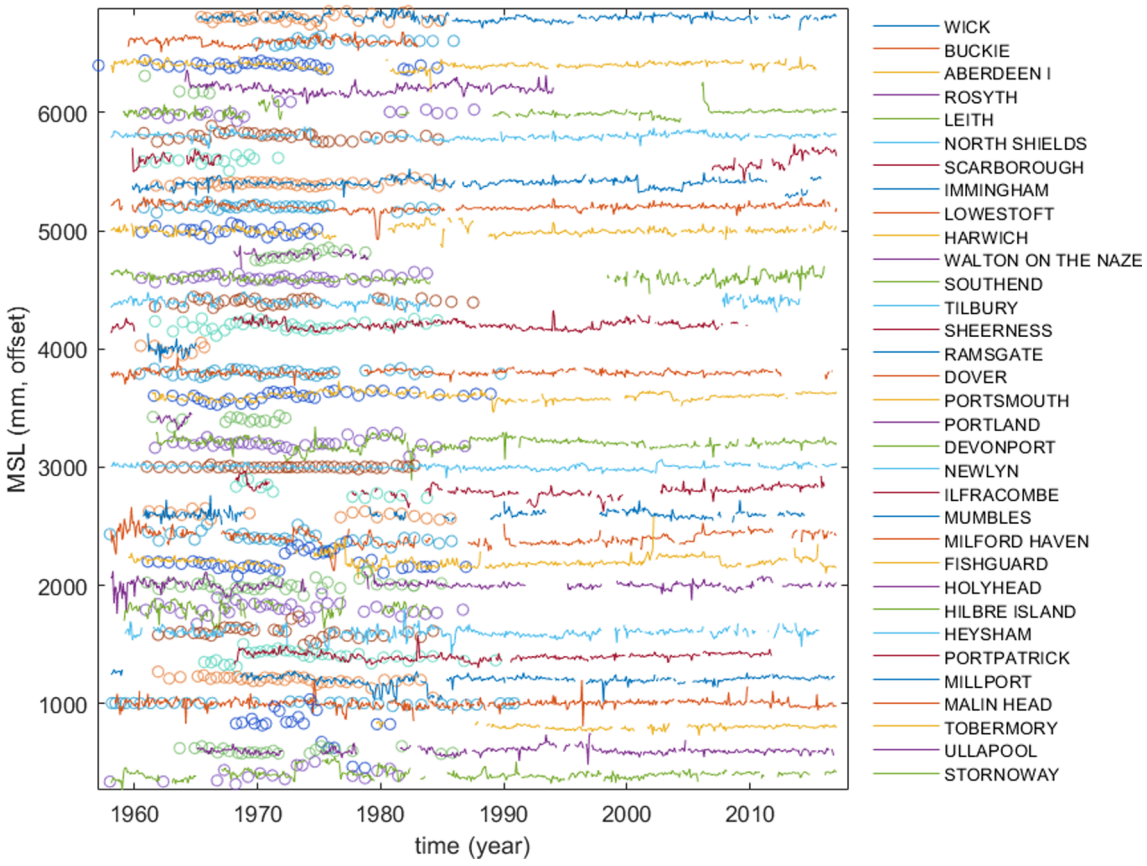

Fig. 8. Data from 33 sites with overlapping TGZ calibration and MSL data. Tide gauge zero calibration results (circles) overlaid on detrended monthly MSL time series with surge model data and common mode subtracted. Inspection shows correlation at interannual timescales implying some lower frequency variability in apparent MSL is due to variability of recorded TGZ setting.

or poor datum control. Belfast in particular displays cm-scale step like discontinuities and nonlinearities which cannot be accounted for using existing metadata. At Islay (42) the SLR curve appears smooth, but the SLR and Sea Level Acceleration (SLA) trends are anomalously high, which can be explained by the jetty subsidence reported by the TGI at this site. Without additional measurements of this subsidence, little can be done to correct the data. For Avonmouth (28), the overall record appears to show anomalously high SLR acceleration, which is likely to be due to one or more unrecorded downward datum shifts in the 1960 s. For Devonport (23), the tide gauge levelling measurements account for all but one large datum step (around 70 mm) associated with a re-siting of the gauge (which would again lead to larger SLR acceleration). This can however be resolved by a single buddy check comparison, as has been done previously over the entire record (Haigh et al., 2009). Despite these issues, apart from Tower Pier (see previously), only Islay and Belfast were judged to be so extreme as not to be used in the overall trend analysis, reducing the number of sites to 46.

Some of the series with slightly less than 20 years of data (analysed but not included in this paper) also show likely symptoms of subsidence or gauge movement, such as Newport (on the other side of the Avon estuary from Avonmouth (28)) and Scarborough (South of Whitby (9)). At Scarborough vertical movement of the structure at the gauge site is the most likely cause of the apparent SLR being higher than at other East Coast sites. This is supported by evidence from a second more recently levelled gauge elsewhere in the harbour (run by the Channel Coastal Observatory), as there is now a vertical offset between MSL data from the two gauges, despite both being originally referenced to the same datum.

6. Results and tests of robustness

6.1. Reduced variability

Despite the overall large month to month MSL variations (Fig. 13), the spread of MSL values (here detrended for linear and quadratic terms) for each month for all sites is considerably reduced compared with uncorrected data. This would be expected if the correction process was effective and the MSL was highly coherent at regional scale over a wide range of frequencies. Fig. 13 shows detrended MSL for all stations overlaid after removal of step offsets, optical density is related to the degree of time series overlap (commonality). The middle trace shows the same data after the CS3X data (from the nearest grid cell) is removed at each station. The bottom plot shows the effect of removing the common mode signal from each time series. Here the median (red), first and third quartile (yellow shading), as well as the maximum and minimum values (grey envelope) are plotted. This suggests that if local meteorological effects (atmospheric pressure and winds, represented by the tide surge model), any large scale variability due to ocean fluctuations (represented by the common mode signal), linear (GIA and SLR) and second order terms (including any SLR and VLM rate changes) are accounted for, then the residual has little remaining variability or higher order terms. Tests confirmed that removing a degree 2 (quadratic) polynomial from each time series reduced temporal aliasing from the different periods of data available at each site rather more than just removing a linear trend, but that adding additional higher order products made little difference to the final result.

The total variance of the original deseasonalised and detrended monthly MSL time series can be viewed as made up of these main components as in Fig. 14.

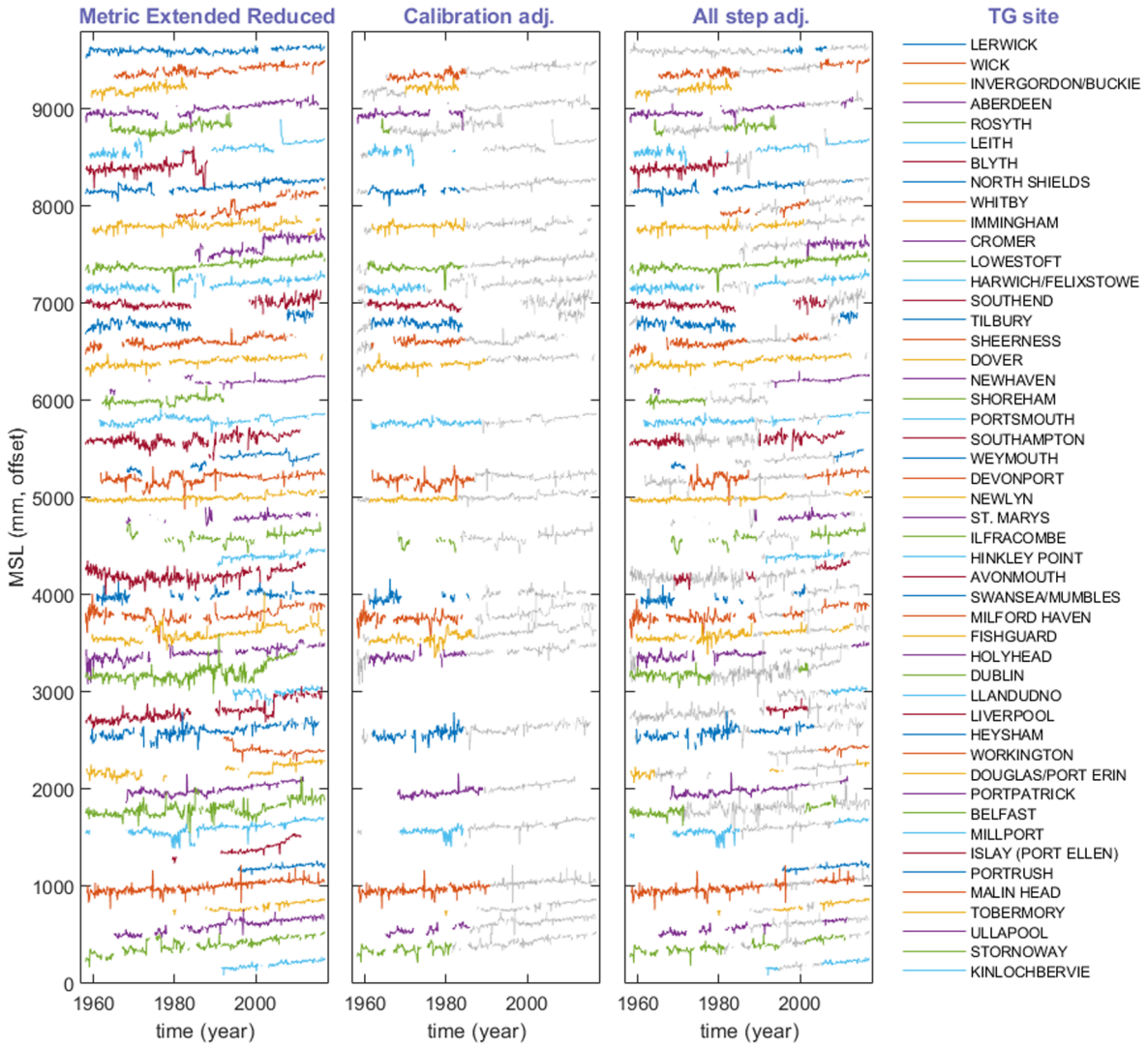

Fig. 9. Metric extended reduced monthly MSL time series for 48 sites with over 20 years of data from Jan. 1958 to Dec. 2018. Left panel: adjusted only for seasonal variation, GIA, surge model data and common mode. Centre panel: data for 28 sites with more than 20 years of data and where TGZ calibration data is available. Calibration corrections are applied to the coloured sections (grey sections are unadjusted at this stage). Right panel: data from all sites, coloured where calibration and documented levelling information are available. These segments are fixed, whilst remaining segments (grey) are adjusted, here using a regression method.

The residual variance (blue) is in many cases smaller than the variance explained by the datum steps (purple), showing that these were the dominant error source at many sites.

The middle and bottom curves of Fig. 13 together demonstrate that, in addition to the removed quadratic trend, there is interannual to interdecadal variability which is common to most of the tide gauge records; i.e. a strong common mode. It is also notable from the bottom curve that the residual variability reduces over the period studied (Fig. 13). Possible explanations include improved data quality (Lennon, 1971) as new gauge technology (Pugh 1972; 1981) replaces older mechanical gauges in the late 1980 s, along with a change to a single data supplying authority, and improved model accuracy as more and higher quality meteorological observations are assimilated into the forcing for the tide and surge model. Another factor is the varying number of gauges contributing, which increases in around 1990, reaching a peak around 2010 after which there is a rapid decline (Fig. 15).

6.2. Constraining step adjustments

Any step removal process runs the risk of artificially removing long period variability. In Fig. 16 we demonstrate that, by only permitting adjustment of "free floating" segments, we minimise this problem in our analysis. The final data (bottom curve) retains the interannual variability of the original data (top), while reducing the scatter around that variability. In contrast, application of a naïve method which automatically corrects all steps above a threshold without regard to independent levelling information (middle curve) results in a significant reduction of this common mode variability.

6.3. Improved trend correlation

Fig. 17 illustrates the improved homogeneity of trends for time series with at least 50 years of data over the Jan. 1958 to Dec. 2018 period after this process of data correction has been applied independently at each site. We selected 50 years as a compromise between maximising the number of sites and ensuring the observations were over a near identical long period to minimise effects of different start or end times. The CATS software is used for all trend analysis. The probability density function (PDF) plot, uses the Epanechnikov smoothing function also available in MATLAB® (Epanechnikov, 1969; Bowman and Azzalini, 1997). Numerical values for the SLR trends and uncertainties for each site are given in supplementary material 1. Due to the presence of coloured noise the uncertainties are larger than if

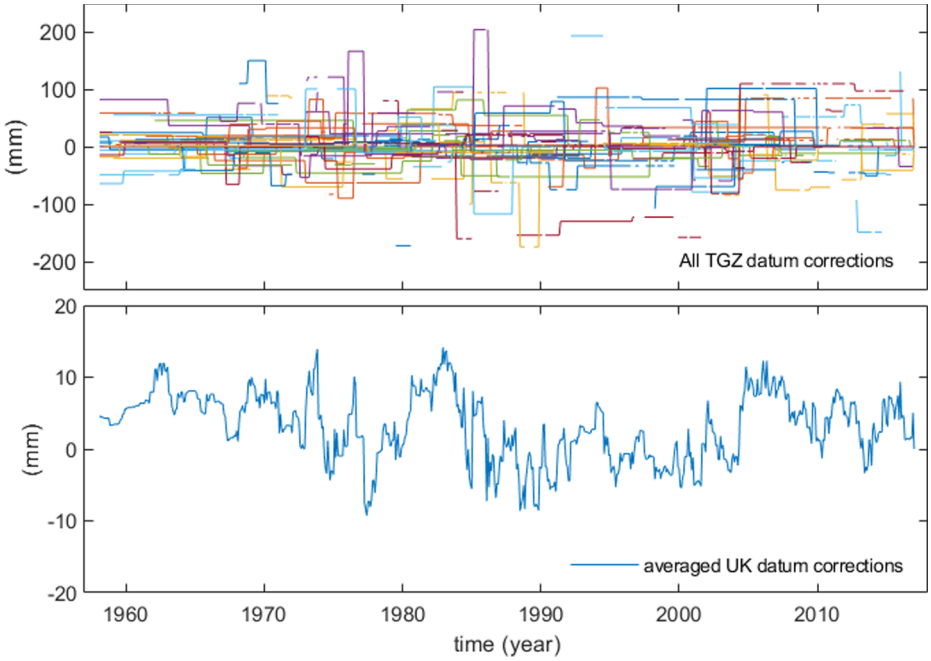

Fig. 10. a and b: Upper panel (a) shows additional offset correction values (to be subtracted from the original data) for each individual site referenced to nominal TGZ, overlaid. Lower panel (b) shows average of all sites (note different vertical scale).

Table 2
SLR and SLA trends derived from CATS, first two columns show linear trend and uncertainty. Third and fouth columns show the second order trend and uncertainty. Table also shows the impact of adjusting MSL series for surge model and different common mode signals prior to averaging. For example the reduction in variability after subtracting an independent "common mode" signal derived from all West coast site data and applying to each East coast site series before averaging shows an additional coherent underlying signal is present around the entire coastline which is not explained by the barotropic model.

Data used for trend analysis	SLR (mm/yr)	σ (mm/yr)	SLA (mm/yr^2)	σ (mm/yr^2)
Average RLR MSL (34 sites)	1.92	0.23	0.085	0.026
Average MER MSL (46 sites)	2.22	0.23	0.077	0.027
ICM (Av. MER minus surge model)	2.30	0.28	0.066	0.030
FCM (Av. MER minus surge model & datum steps)	2.39	0.27	0.056	0.028
Av. MER: as above, 4 longest series only	2.39	0.36	0.049	0.038
FCME (E. Coast MER only) minus detrended FCM	2.21	0.05	0.073	0.006
FCMW (W. Coast MER only) minus detrended FCM	2.54	0.06	0.066	0.007
FCMS (S. Coast MER only) minus detrended FCM	1.89	0.10	0.054	0.011
FCME minus detrended FCMW	2.26	0.10	0.071	0.011
FCME minus detrended FCMS	2.20	0.12	0.070	0.011
FCMW minus detrended FCMS	2.47	0.16	0.065	0.017

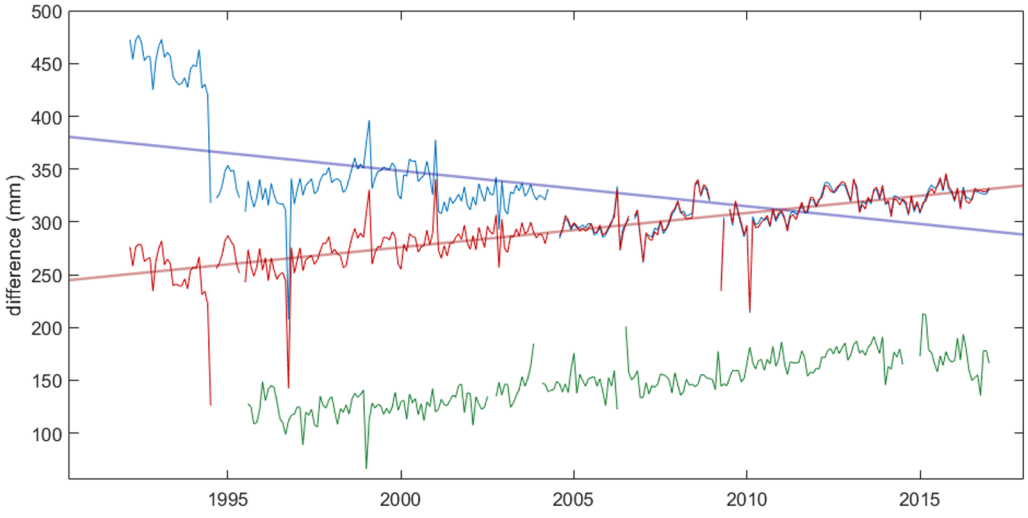

Fig. 11. Monthly MSL for Workington (blue), adjusted for seasonal variation, GIA, meteorological variability and Initial Common Mode, showing three distinct steps, which contribute to a linear trend of -4.2 mm yr^{-1} . Red: result after step adjustment based on regression, with a revised trend of 2.4 mm yr^{-1}. Green: Unadjusted record for Portrush (offset) shown for comparison. (For interpretation of the references to colour in this figure legend, the reader is referred to the web version of this article.)

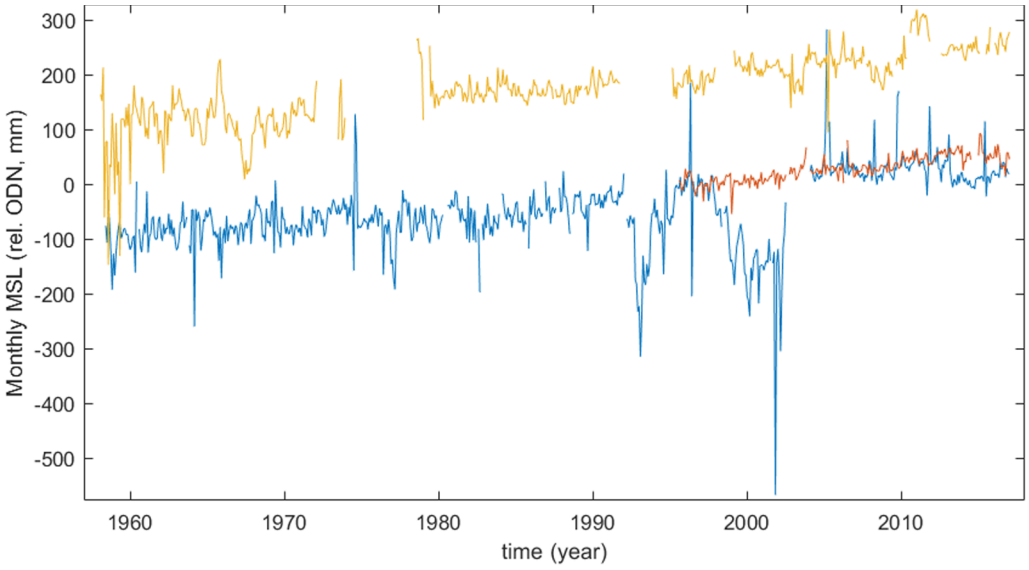

Fig. 12. Monthly MSL for Malin Head (blue) and Portrush (red), and Holyhead (orange), distance 46 km and 288 km from Malin Head respectively, all to relevant OD. The data from Portrush can be used to replace part of the erroneous data from Malin Head. The new composite series appears to be consistent with those from several other sites. (For interpretation of the references to colour in this figure legend, the reader is referred to the web version of this article.)

white noise is assumed (Bos et al., 2013).

Note that, while the correction of "free floating" data segments will tend to reduce interannual variability, it is not biased in its representation of either linear or quadratic trend, which could be made less consistent with other records if the method was not effective. The improvement overall suggests that there are sufficient segments with levelling data to constrain the curves well. The results are consistent with the idea of uniform regional long term underlying trends and low order decadal and multi-decadal variability having long spatial coherence lengths and therefore being highly correlated along coastlines at regional scale (Hughes and Meredith, 2006; Woodworth et al., 2009; Wahl et al., 2013; McCarthy et al., 2015). They show that, although GIA is important, the correction of steps has the greatest impact on unifying observed trends around the coast.

As a check of whether the corrections are still valuable over the later period when much less levelling information is available, we compare trends over the 1993–2017 period with those from satellite altimetry (Pfeffer and Allemand, 2016; Kleinherenbrink et al., 2018), choosing either the nearest altimetry grid point or an average over all points within around 100 km of each gauge. Note that we take care to match the GIA corrections, applying a correction for both vertical land movement and gravity at the tide gauges, but only the gravity effect for the altimetry. Fig. 18 confirms that the corrections improve consistency with satellite altimetry over this period.

6.4. Revised MSL for the British Isles

We now construct the Final Common Mode (FCM) from the time series after correction for steps, this time retaining both linear and quadratic trends. Simple averaging presents a problem as offsets between series exist (each series is not referenced to the same absolute vertical datum) and they do not cover the same time period (Dangendorf et al., 2017). Any GIA errors will also cause apparent trend differences and introduce bias. The novel averaging process used here is to solve for all offsets in all time series simultaneously using weighted least squares in Matlab, accounting for data gaps and differing start and

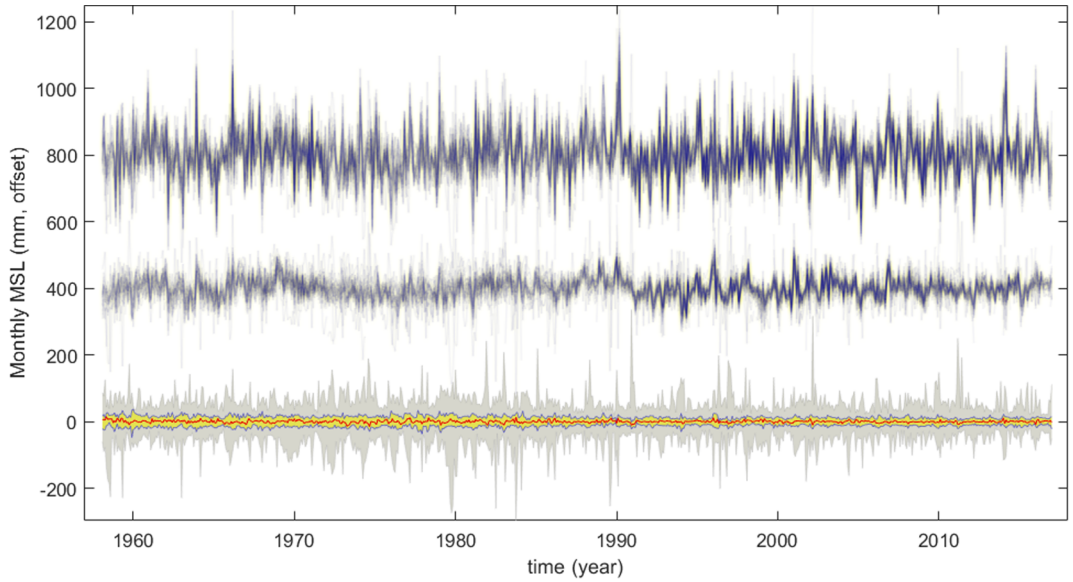

Fig. 13. Top trace, overlaid detrended (1st and 2nd order), deseasonalised MSL time series with mean offset removed for all sites. Optical density is proportional to number of coincident time series. Middle trace is the same but with storm surge model removed for each site. Bottom trace is with common mode signal removed, and median, 1st and 3rd quartile as well as max/min envelope shown.

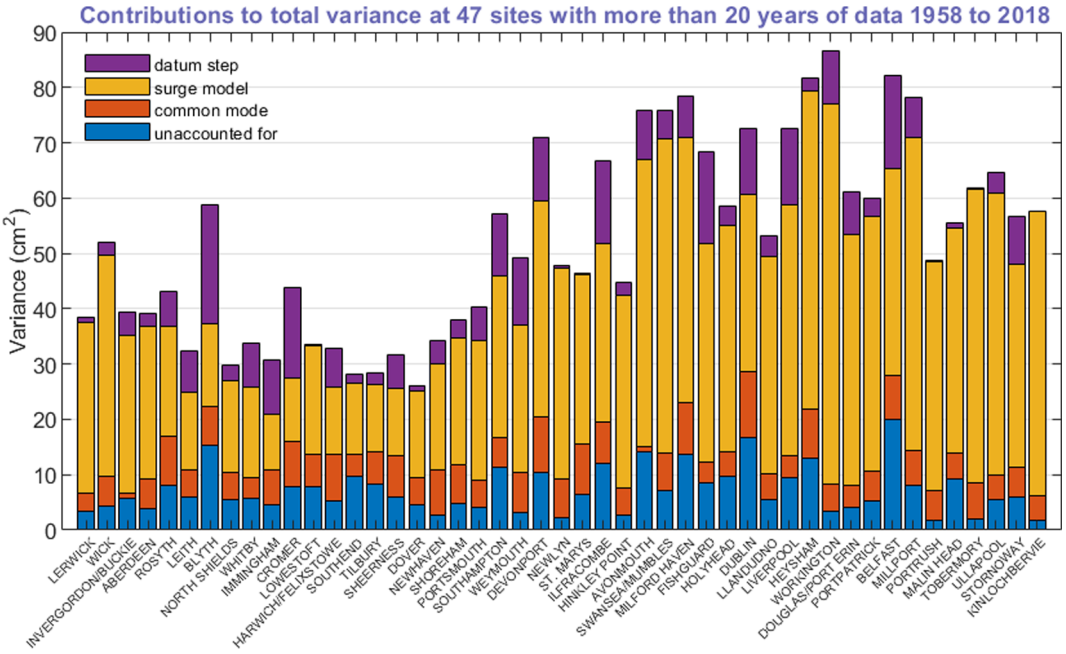

Fig. 14. Contributions to total variance of deseasonalised monthly mean MSL at each site. The smaller contribution of the surge model and lower variance on the East and South-East Coasts reflect wind driven processes. The difference is similar to the results found between the East Coast of the UK and the Western European Coast using low pass filtered data (Frederikse et al. 2018).

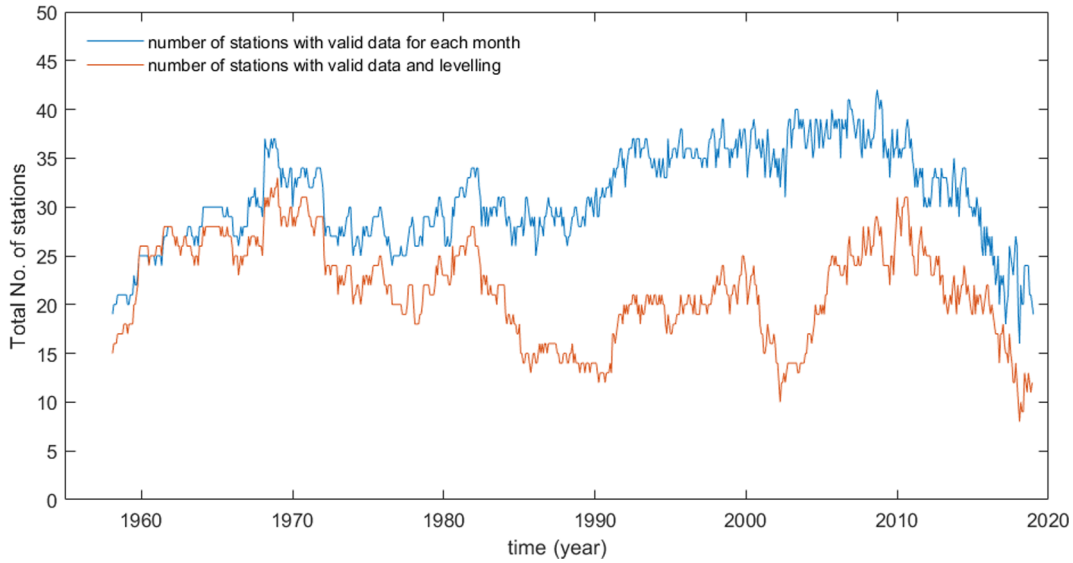

Fig. 15. Blue: total number of sites with valid MSL data per month Jan. 1958 to Dec. 2017. Red: The number of these sites which also have robust levelling information. (For interpretation of the references to colour in this figure legend, the reader is referred to the web version of this article.)

end times, but in this paper we do not attempt to account for GIA errors. We check this averaging is effectively identical to an alternative process of ranking the time series in length order, and then starting with the longest and most complete, to sequentially add each new series to update an overall average. At each stage the offset between the current average and each new series is estimated by least squares differences and this offset is then subtracted before creating a new weighted average. In both cases the average at each point in the time series is weighted by the number of contributing gauges.

Fig. 19 shows all of the adjusted and offset time series overlaid. The amount of direct curve overlap is visually represented by optical density, with a median, 1st and 3rd quartile plotted. The common mode variability is clearly evident.

Subtracting the surge model data results in greatly reduced high frequency variability in the average MSL data, but makes little difference to the formal trend (using CATS processing to account for power law noise models, the formal uncertainty actually increases slightly as a result of reduced white noise permitting a better estimate of the low frequency noise, see Table 2).

Fig. 20 shows the variation in trend differences between the FCM and the MSL at each of the TG stations with more than 20 years of data. Each TG difference trend is estimated over the timespan of each TG record. Possible contributors to the residual trend differences include GIA model errors and VLM (see Fig. 22) as well as any remaining gauge errors.

6.5. Sea level acceleration

The question arises whether acceleration is detectable in the adjusted dataset. The minimum record length required in order to attempt

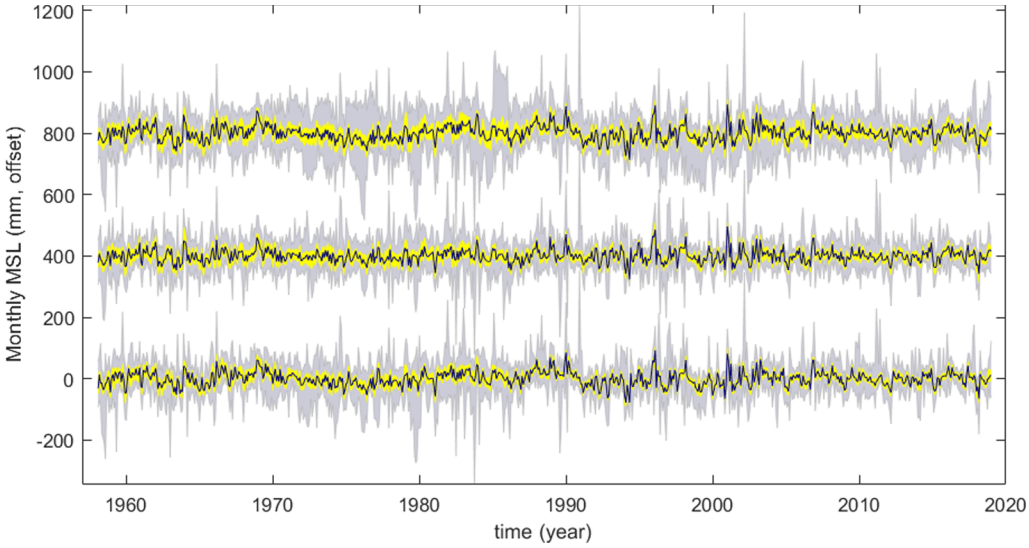

Fig. 16. Top trace, overlaid detrended (1st and 2nd order), deseasonalised unadjusted MSL with mean offset and storm surge model data removed for all sites. Median, 1st and 3rd quartile as well as max/min envelope shown. Middle trace is the same but with detected steps removed using maximum likelihood change detection. Note some low frequency variations are also removed from the mean. Bottom trace is with datum steps removed using levelling data and event time regression. Note low frequency variability is retained whilst envelope and interquartile spread are reduced to similar levels as middle trace. Each trace is offset 400 mm for visualisation.

separation of interdecadal ocean fluctuations from a long term acceleration signal in tide gauge data is much longer than the 20 years used here for SLR (Douglas, 1992). In Fig. 21, a probability density function of CATS derived acceleration values is plotted using all 24 gauges with at least 50 years of data (at least 75% complete). This shows a median acceleration of around 0.05 mm yr^{-2} over the Jan. 1958 to Dec. 2018 period, and a greatly reduced spread of values around a positive mean compared with unadjusted data, indicating an increased likelihood of a positive acceleration signal.

This illustrates the improved consistency of the tide gauge records once datum steps and local dynamics have been accounted for. However, similar time series will result in similar estimates of acceleration without that acceleration necessarily being statistically significant. To assess the accuracy of trends and accelerations, we apply the CATS analysis method to various Common Modes defined below (Table 2). The linear trends (SLR given by b) are derived accounting for a second order term (Williams et al., 2014) using (1).

$$y = a + b(t - t_0) + \frac{1}{2}c(t - t_0)^2 \quad (1)$$

where y is sea level, a is a constant, b is the rate of rise, and c is the acceleration. We select t_0 so that b equals the derived trend in a linear fit over the full period Jan. 1958 to Dec. 2018, making b equivalent to the value which would be estimated with no acceleration term. This selection is done iteratively starting at the middle of the time series. This reduces the linear trend uncertainty in all cases considered here.

In order to test the robustness of our methodology, we also calculated three independent Common Modes based on tide gauges from the West, East and South coasts of the UK: FCMW, FCME and FCMS (similar to the method used for Fig. 9 in Woodworth et al., 1999). The FCM, and the differences between the local FCMs and the full FCM, are plotted in Fig. 22. The West coast here includes gauges from the Irish coast, and we also use four additional sites where the records have 75% completeness over a minimum 20 years, to maximise the sample number. These independent constructions, plus other tests such as using (or omitting) the small number of tide gauges with long and almost complete records, or constructing the FCM ignoring all “free floating” data segments (not shown), demonstrate the robustness of the FCM and of the procedure for correcting steps. The residual small linear and second order trend differences (Fig. 22; orange, red, purple) are suggestive of VLM changes and this could be investigated in further work (e.g. using CGPS compared with GIA models, Bingley et al., 2001; Teferle et al., 2002; Santamaría-Gómez et al., 2017).

The resulting quadratic fit parameters and their errors are shown in Table 2, where the linear component should be interpreted as the rate

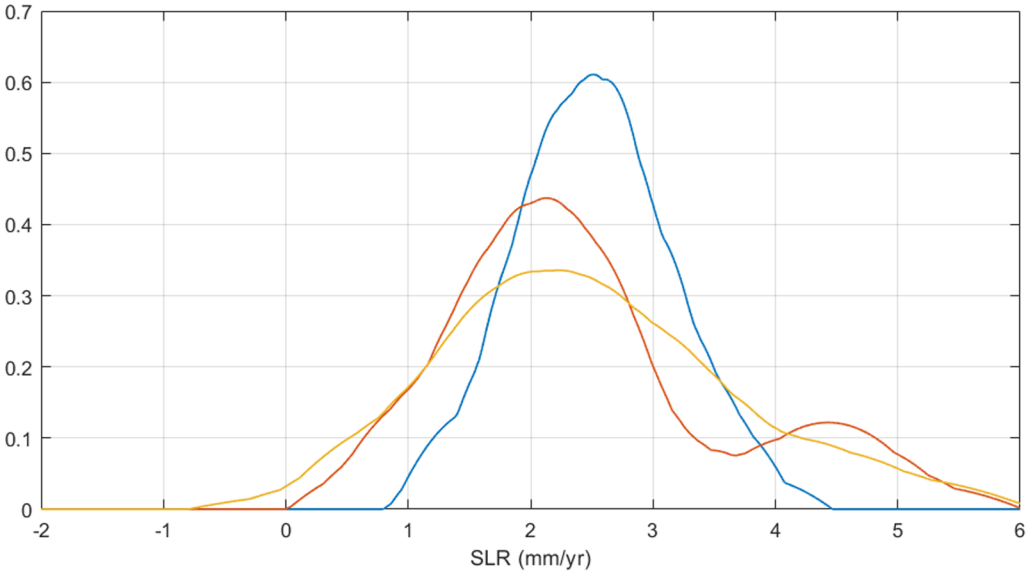

Fig. 17. PDF of SLR trends from 24 sites with more than 50 years of monthly MSL data and 75% completeness. Yellow: only GIA correction applied. Red: GIA and storm surge model correction and Initial Common Mode applied. Blue: GIA, tide and surge model plus ICM, and step corrections applied. (For interpretation of the references to colour in this figure legend, the reader is referred to the web version of this article.)

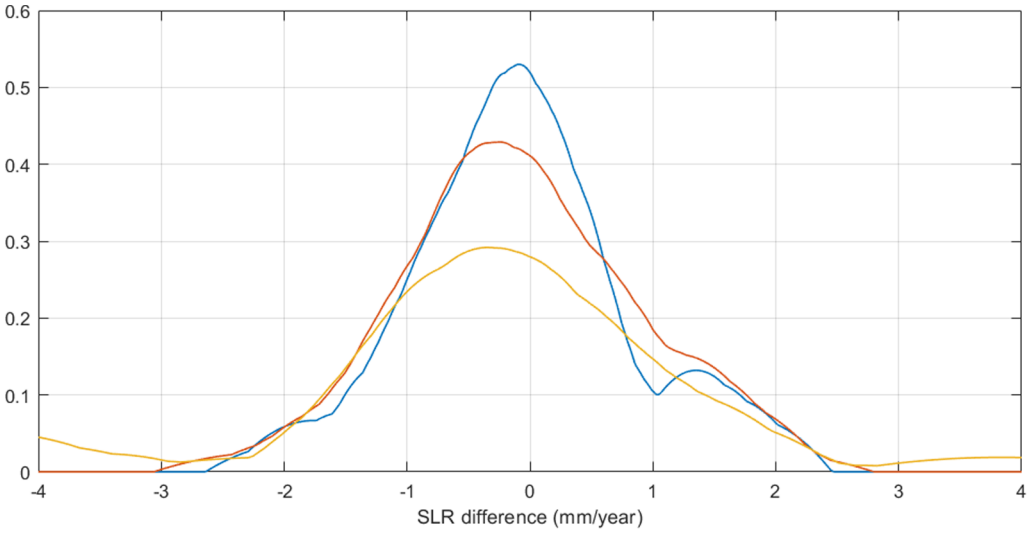

Fig. 18. PDF plots of deseasonalised and GIA corrected MSL trend differences, tide gauge minus multi-mission satellite altimetry for 30 sites around the British Isles which have at least 20 years of data available over the altimetry time period (1993 to 2017). The tide gauge data is adjusted for storm surge and common mode signal. Orange: difference of TG (adjusted for storm surge and common mode signal but without datum steps removed) and nearest altimeter grid cell trends. Red: same as previous but with TG offset adjustments applied. Blue: Difference of TG (adjusted for storm surge, common mode signal and datum steps) and average of nearest 55 altimetry grid cells. (For interpretation of the references to colour in this figure legend, the reader is referred to the web version of this article.)

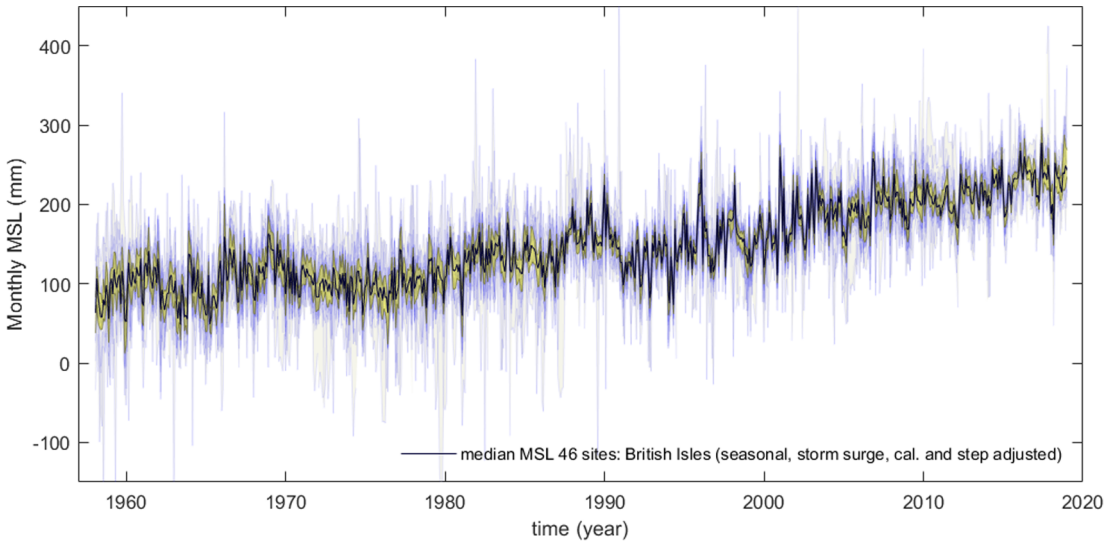

Fig. 19. MSL all sites overlaid. Adjusted for GIA, seasonal effects, and local tide and storm surge, each series (blue in background) offset to weighted average signal. Median MSL from all sites (dark blue), 25th and 75th quartile limits (yellow) and light grey is max/min envelope of data from all sites including outliers. (For interpretation of the references to colour in this figure legend, the reader is referred to the web version of this article.)

in the middle of the period of analysis (start of 1988). We see that the average rate is around 2.4 mm yr^{-1} with around 10% error, and the acceleration is around 0.06 mm yr^{-2}, with around 50% error (without the correction for offset steps, and local dynamics, a slightly larger acceleration is seen). This latter error is dominated by the presence of low frequency variability in the FCM, as can be seen from the significantly smaller uncertainty in acceleration for the difference between the independent FCME and FCMW.

6.6. Comparison with previous work

This revised estimate of regional MSL acceleration around the British Isles is comparable with our calculation of a CATS derived result from the global MSL reconstruction of Church and White (2011), (CW11, 2015 update) of 0.055 $\pm$ 0.013 mm yr^{-2} re-calculated for the 1958 to 2013 period. It is also close to both the global (1958–2015) and the subpolar North Atlantic accelerations for the slightly different period of 1968–2015 calculated by Dangendorf et al. (2019), which are 0.058 and 0.06 $\pm$ 0.01 mm yr^{-2} respectively. This is much higher than the figure of 0.013 $\pm$ 0.003 mm yr^{-2} estimated for the entire CW11 period since 1880, or the estimate of 0.011 mm yr^{-2} (Woodworth et al., 2009) for the UK sea level acceleration over a similarly long period, although it is only marginally higher then the global CW11 acceleration for a more equivalent 55 year period centred on 1931. The global linear trend estimate (SLR) for updated CW11 for the period 1958 to 2013 is also comparable (2.17 $\pm$ 0.12 mm yr^{-1}, the uncertainty is again reduced if the second order term is also accounted for). There are good reasons, such as the influence of the Greenland Ice Sheet, why the acceleration might not match either the global or North Atlantic accelerations over multidecadal timescales, but we do not investigate this here.

If we wish to improve the estimate of acceleration, we must reduce the impact of this low frequency variability either by seeking longer time series (Hogarth, 2014; Haigh et al., 2014), or by finding a physical cause (assuming that to be separable from the long term sea level rise), and subtracting it out.

6.7. Investigating causes of the common mode

Our initial hypothesis was that we should expect a Common Mode

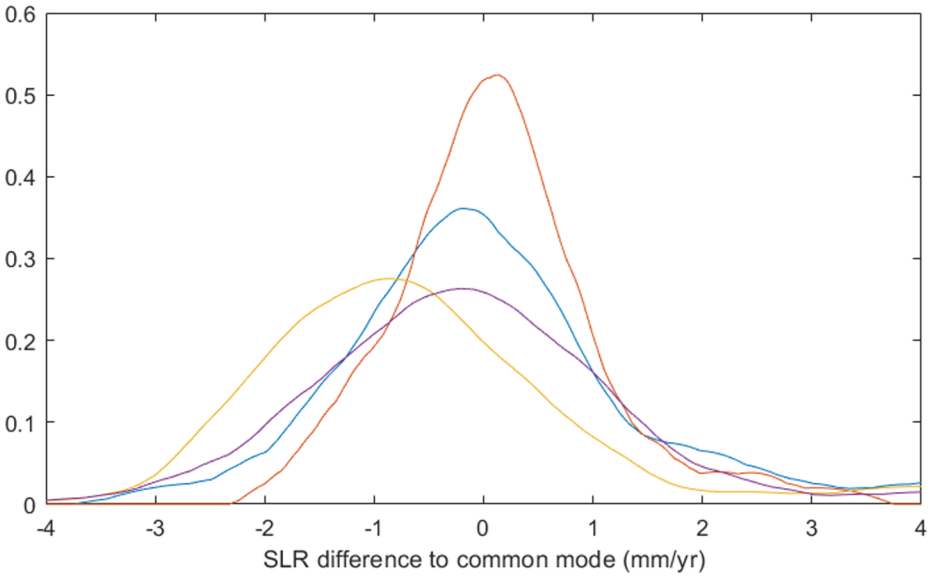

Fig. 20. PDF of CATS derived trend of differences of deseasonalised MSL; all stations with greater than 20 years of data minus the Final Common Mode signal from Fig. 19 (i.e. trends retained). This method accounts for variations in trend over different time periods due to the low frequency variability or acceleration. Red: GIA adjusted MSL, storm surge and offsets subtracted. Blue: GIA adjusted MSL with storm surge only removed. Purple: GIA adjusted MSL. Orange: MSL with no GIA adjustment. (For interpretation of the references to colour in this figure legend, the reader is referred to the web version of this article.)

to reflect the influence of ocean dynamics from beyond the continental shelf, as well as mean sea level rise. We test this by correlating the FCM with satellite altimetry everwhere (with seasonal signals and trends removed). The result, shown in Fig. 23, clearly shows that the FCM is related to eastern boundary Atlantic dynamics, which have previously been attributed to the response to longshore wind stress integrated from the equator (Calafat et al., 2012; Calafat and Chambers, 2013). The link to the basinwide Greenland-Iceland-Norwegian (GIN) sea response further north is consistent with the same effect exciting a pan-Arctic sea level oscillation, the mechanism for which has been elucidated by Fukumori et al. (2015). Thus, if we wish to explain the FCM, a response to longshore winds would be the first place to look. We intend to explore this issue further in future work, and also consider other contributing factors (Roberts et al., 2016). Promising correlations are also seen with sea surface temperature over the entire 60-year period, over a wide region (not shown).

It is worth noting that a very similar correlation pattern emerges if we use the FCME, based on the UK east coast, despite the fact that the altimetry correlations along the east coast are low. This is presumably because the local dynamics have not been subtracted from the altimetry here, and these contain a component which is anticorrelated with the FCM on the east coast.

7. Summary and conclusion

Removing local dynamical effects from British Isles tide gauge measurements based on a barotropic, local shelf sea model, and then constructing a “Common Mode” by averaging the residual signals and removing that, has permitted us to identify a number of previously unrecognised steps in the tide gauge record.

In response to this, an intensive data archaeology exercise has allowed:

- Extension of existing tide gauge datasets using archived bench mark and datum information.
- Collation and digitisation of metadata detailing instrumentation changes at each site.
- Centimetre scale corrections to a number of site datum connections from archived tide gauge calibration data.

These extended and corrected datasets have further allowed:

- Confirmation that most of the steps coincide with recorded instrumentation changes.
- A correction for the steps which in most cases is based on

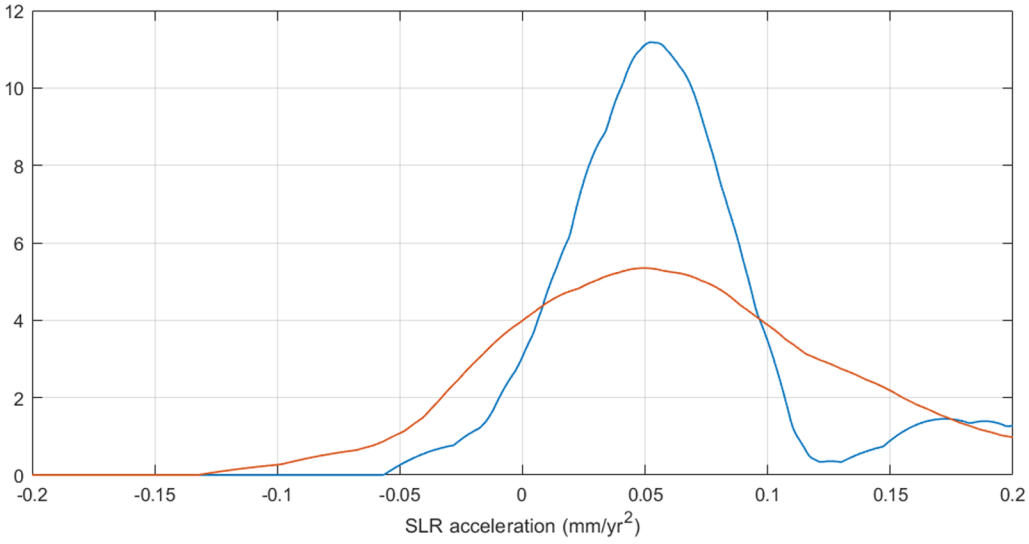

Fig. 21. PDF of acceleration values for 24 sites with data having more than 50 years of data with 75% completeness. Blue: fully adjusted. Red: unadjusted (deseasonalised only) data, showing reduced spread of values once offsets are removed. (For interpretation of the references to colour in this figure legend, the reader is referred to the web version of this article.)

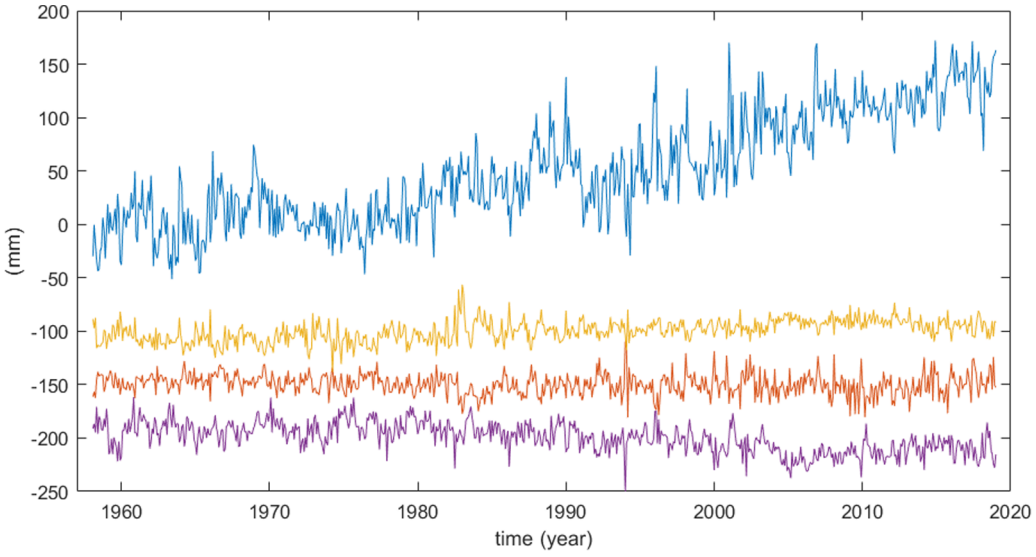

Fig. 22. Top, Blue: Average monthly MSL signal for 46 sites around the British Isles after adjustment for GIA, seasonal variation, and local meteorological effects from a tide and surge model. This is the final "common mode" (FCM) signal with trends retained. Orange: West Coast Common Mode (21 sites) minus the average common mode. Red: East Coast Common Mode (16 sites) minus average. Purple: South Coast Common Mode (9 sites) minus average. The low frequency variations such as the 1988 excursion and sharp drop just after 1990 are robust features of the reanalysed MSL data. Series are offset to aid visualisation. (For interpretation of the references to colour in this figure legend, the reader is referred to the web version of this article.)

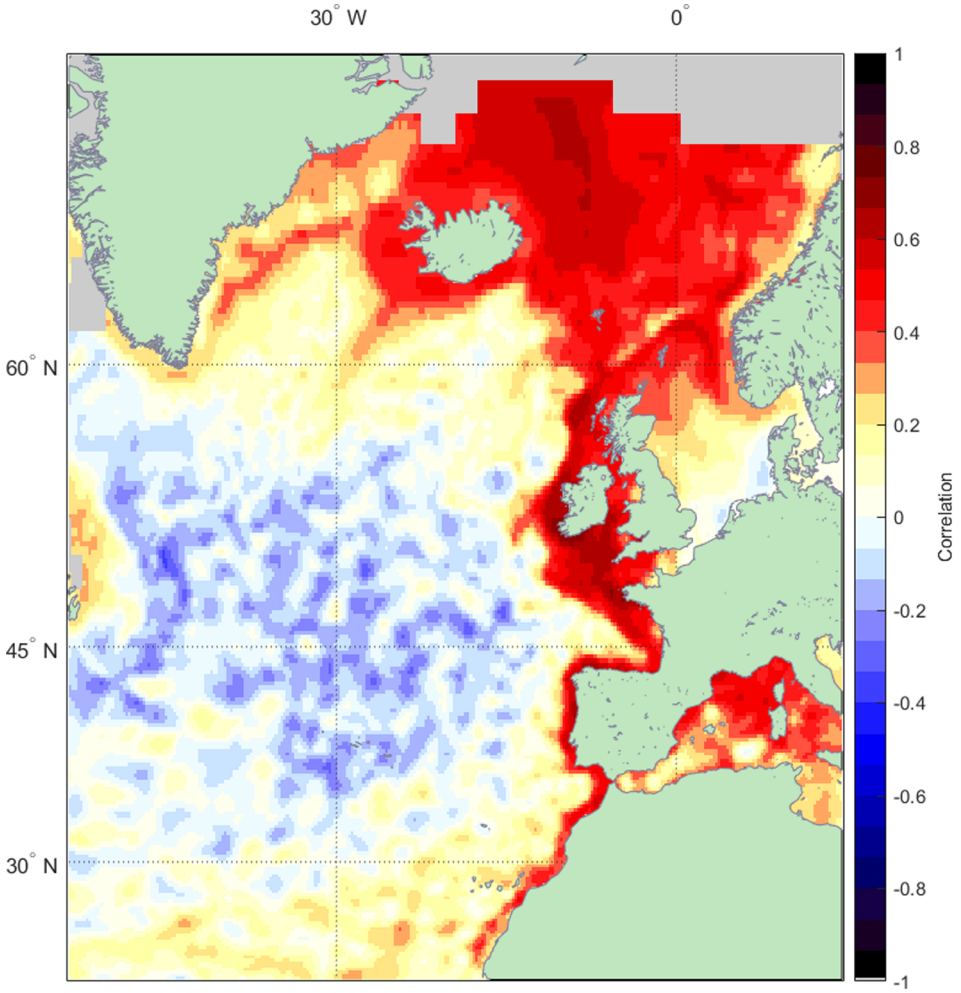

Fig. 23. Correlation of detrended final common mode signal (FCM, average of MSL around the British Isles after offsets, storm surge model data and seasonal components are removed) with detrended and deseasonalised satellite altimetry data. This pattern is robust even if only tide gauge data from the UK east coast is used to create the common mode signal.

documented levelling measurements.
- Consequent reduction in low frequency variability at many individual sites.
- Reduced variance between site data, with coherent interannual patterns at local scale.
- Increased correlation of rates and accelerations of sea level rise at all sites.

The effect of estimating and removing the tide gauge zero offset steps is to both increase the overall correlation between data from all sites and to reduce the variability at each site. A large number of the newly adjusted time series now appear similar to each other and to time series from the handful of sites where the RLR data was previously assessed as high quality (such as Lowestoft or Newlyn). The correlation between MSL trends adjusted using a GIA model at different sites as well as between Altimeter and TG MSL records and trends is also improved. These results do not substantially alter the SLR picture obtained previously using selected RLR PSMSL data, but they do greatly increase confidence in the conclusions, and allow problematic sites to be identified or even rehabilitated more easily.

The new average MSL signal is similar in concept to the longer-term UK "Sea Level Index", (Woodworth et al., 2009) after the tide and storm surge (meteorological) variability and datum steps have been removed (Fig. 22, top trace). This Final Common Mode variability shows a mean sea level rise of 2.39 ± 0.27 mm yr^{-1}, and an acceleration of 0.058 ± 0.030 mm yr^{-2} between the start of 1958 and the end of 2018 (N.B. the linear rates are corrected for GIA using the ICE-6G_C (VM5a) model as described in the data section above). The central estimate implies a rate rising from 0.33 mm yr^{-1} at the start of the record to 4.11 mm yr^{-1} by the end, with an average rate over the satellite altimetry period (start of 1993 to the end of 2017) of 3.46 mm yr^{-1}. This is consistent with the recently reported global acceleration over the altimetry era of 0.084 ± 0.029 mm yr^{-2} (Nerem et al., 2018), and much stronger than the typical 0.01 mm yr^{-2} acceleration observed over century time scales (Hogarth, 2014).

Comparison with satellite altimetry (Fig. 23) shows that the Common Mode is linked to eastern Atlantic boundary variability. It may be possible to reduce error bounds on the underlying acceleration if a model for the wind-driven component of these boundary signals can be used to reduce the interannual to decadal variability seen in the Common Mode.

This reassessment and improved consistency of the tide gauge records relied heavily on the existence of redundant tide gauge measurements and of levelling information which constrains the "free floating" segments of the records. Many of the steps we detected are subsequently reversed as later levelling reasserts the correct datum following some earlier equipment change. In this context, the recent drop off in the number of usable tide gauge records and in levelling to nearby datums (Fig. 15) is alarming as, without this combination of redundancy and levelling, the quality of reconstruction of the common mode is likely to degrade into the future, limiting our ability to detect future accelerations.

It is also pertinent to assess data from some of the recently installed radar tide gauges which are not covered in this analysis (as they have been running less than 20 years). An initial examination of some of the longer radar gauge records indicates that despite the intrinsic stability of such gauges (Woodworth and Smith, 2003) unrecorded datum changes are still evident. For example, for the almost continuous 2006 to 2018 record from Deal Pier (approx. 15 km N.E. of Dover) two datum steps of around −40 mm are identified at mid-2011 and the end of 2013 by the buddy check and model difference methods. These lead to an uncorrected (and clearly erroneous) trend of −7.9 mm yr^{-1}, whilst the adjusted trend after the processing steps outlined here gives 2.2 mm yr^{-1}. Unfortunately, no physical changes are recorded in the available site documentation.

A broader implication of this work is that additional levels of quality control should be considered before drawing conclusions about SLR from regions where only small numbers of gauges are available.

8. Data availability

A processed data set and associated metadata is available online through Zenodo at: https://doi.org//10.5281/zenodo.3747196

The data is available in .csv spreadsheet format and also as MATLAB® .mat format files, the .mat files are simple 2-D data arrays where columns 1 to 1351 correspond to the PSMSL site id. number, and rows 1 to 3228 correspond to months from Jan. 1750 to Dec. 2018.

Declaration of Competing Interest

The authors declare that they have no known competing financial interests or personal relationships that could have appeared to influence the work reported in this paper.

Acknowledgements

This paper contains work conducted during a PhD study supported by the Natural Environment Research Council (NERC) EAO Doctoral Training Partnership and is fully-funded by NERC whose support is gratefully acknowledged. Grant ref no is NE/L002469/1, UKRI award ref 1950000.

All code used in this research was developed using MATLAB® release 2019a.

MATLAB® is a registered trademark of The MathWorks, Inc., Natick, Massachusetts, United States.

Thanks to: P. L. Woodworth for useful comments on earlier versions. The authors also thank the three reviewers whose comments have further improved the paper. We also acknowledge the many contributors to on-line MATLAB® forums who have provided inspiration for more efficient coding solutions. Maps in MATLAB® were created using:

Pawlowicz, R. (2019). "M_Map: A mapping package for MATLAB", version 1.4 k, [Computer software], available online at www.eoas.ubc.ca/~rich/map.html.

Peter Kovesi. Good Colour Maps: How to Design Them. arXiv:1509.03700 [cs.GR] 2015

Appendix A. Supplementary material

Supplementary data to this article can be found online at https://doi.org/10.1016/j.pocean.2020.102333.

References

Aarup, T., Merrifield, M. A., Pérez, B., Vassie, I., & Woodworth, P. L. (2006). Manual on Sea Level Measurement and Interpretation. Volume IV: An update to 2006. Intergovernmental Oceanographic Commission Manuals and Guides. Paris: Intergovernmental Oceanographic Commission of UNESCO.

Argus, D.F., Peltier, W.R., Drummond, R., Moore, A.W., 2014. The Antarctica component of postglacial rebound model ICE-6G_C (VM5a) based upon GPS positioning, exposure age dating of ice thicknesses, and relative sea level histories. Geophys. J. Int. 198 (1), 537–563. https://doi.org/10.1093/gji/ggu140.

Beaulieu, C., Chen, J., Sarmiento, J.L., 2012. Change-point analysis as a tool to detect abrupt climate variations. Philos. Trans. Royal Soc. A Math Phys. Eng. Sci. 370 (1962), 1228–1249.

Becker, M., Karpytchev, M., Davy, M., Doekes, K., 2009. Impact of a shift in mean on the sea level rise: Application to the tide gauges in the Southern Netherlands. Cont. Shelf Res. 29 (4), 741–749.

Bingley, R., Dodson, A., Penna, N., Teferle, N., Baker, T., 2001. Monitoring the vertical land movement component of changes in mean sea level using GPS: results from tide gauges in the UK. J. Geospatial Eng. 3 (1), 9–20.

Bos, M.S., Williams, S.D.P., Araújo, I.B., Bastos, L., 2013. The effect of temporal correlated noise on the sea level rate and acceleration uncertainty. Geophys. J. Int. 196 (3), 1423–1430.

Bowman, A.W., Azzalini, A., 1997. Applied smoothing techniques for data analysis. Oxford University Press Inc, New York.

Bradley, S.L., Milne, G.A., Shennan, I., Edwards, R., 2011. An improved glacial isostatic adjustment model for the British Isles. J. Quaternary Sci. 26 (5), 541–552.

Bradshaw, E., Woodworth, P.L., Hibbert, A., Bradley, L.J., Pugh, D.T., Fane, C., Bingley, R.M., 2016. A century of sea level measurements at Newlyn Southwest England. Mar. Geod. 39 (2), 115–140.
Calafat, F.M., Chambers, D.P., Tsimplis, M.N., 2012. Mechanisms of decadal sea level variability in the eastern North Atlantic and the Mediterranean Sea. J. Geophys. Res. Oceans, 117(C9). https://doi.org/10.1029/2012JC008285.
Calafat, F.M., Chambers, D.P., 2013. Quantifying recent acceleration in sea level unrelated to internal climate variability. Geophys. Res. Lett. 40 (14), 3661–3666.
Carrère, L., Faugère, Y., Ablain, M., 2016. Major improvement of altimetry sea level estimations using pressure-derived corrections based on ERA-Interim atmospheric reanalysis. Ocean Sci 12, 825–842.
Caussinus, H., Mestre, O., 2004. Detection and correction of artificial shifts in climate series. J. Roy. Stat. Soc.: Series C (Appl. Statistics) 53 (3), 405–425. https://doi.org/10.1111/j.1467-9876.2004.05155.x.
Chafik, L., Nilsen, J.E.Ø., Dangendorf, S., Reverdin, G., Frederikse, T., 2019. North Atlantic Ocean circulation and Decadal Sea level change during the Altimetry Era. Sci. Rep. 9 (1), 1041.
Church, J.A., White, N.J., 2011. Sea-level rise from the late 19th to the early 21st century. Surv. Geophys. 32 (4–5), 585–602. https://doi.org/10.1007/s10712-011-9119-1.
Dangendorf, S., Calafat, F.M., Arns, A., Wahl, T., Haigh, I.D., Jensen, J., 2014. Mean sea level variability in the North Sea: Processes and implications. J. Geophys. Res. Oceans 119 (10). https://doi.org/10.1002/2014JC009901.
Dangendorf, S., Marcos, M., Wöppelmann, G., Conrad, C.P., Frederikse, T., Riva, R., 2017. Reassessment of 20th century global mean sea level rise. Proc. Natl. Acad. Sci. 201616007. https://doi.org/10.1073/pnas.1616007114.
Dangendorf, S., Hay, C., Calafat, F.M., Marcos, M., Piecuch, C.G., Berk, K., Jensen, J., 2019. Persistent acceleration in global sea-level rise since the 1960s. Nat. Clim. Change. https://doi.org/10.1038/s41558-019-0531-8.
Doodson, A.T., 1924. Meteorological perturbations of sea-level and tides. Geophys. J. Int. 1, 124–147.
Douglas, B.C., 1992. Global sea level acceleration. J. Geophys. Res. Oceans 97 (C8), 12699–12706.
Eckley, I.A., Fearnhead, P., Killick, R., 2011. Analysis of changepoint models. Bayesian Time Series Models 205–224.
Emery, K.O., Aubrey, D.G., 1985. Glacial rebound and relative sea levels in Europe from tide-gauge records. Tectonophys. 120 (3–4), 239–255.
Epanechnikov, V.A., 1969. Non-parametric estimation of a multivariate probability density. Theory Probability Its Appl. 14 (1), 153–158.
Feuerstein, D., Parker, K.H., Boutelle, M.G., 2009. Practical methods for noise removal: applications to spikes, nonstationary quasi-periodic noise, and baseline drift. Anal. Chem. 81 (12), 4987–4994.
Flather, R.A., Heaps, N.S., 1975. Tidal Computations for Morecambe Bay. Geophys. J. Int. 42 (2), 489–517. https://doi.org/10.1111/j.1365-246X.1975.tb05874.x.
Flather, R.A., 1981. Results from a model of the north east Atlantic relating to the Norwegian Coastal current. In: Saetre, R., Mork, M. (Eds.), The Norwegian Coastal Current. Bergen University, pp. 427–458.
Flather, R.A., 2000. Existing operational oceanography. Coast. Eng. 41 (1), 13–40. https://doi.org/10.1016/S0378-3839(00)00025-9.
Flowerdew, J., Horsburgh, K., Wilson, C., Mylne, K., 2010. Development and evaluation of an ensemble forecasting system for coastal storm surges. Q. J. R. Meteorolog. Soc. 136 (651), 1444–1456. https://doi.org/10.1002/qj.648.
Frederikse, T., Riva, R., Slobbe, C., Broerse, T., Verlaan, M., 2016a. Estimating decadal variability in sea level from tide gauge records: An application to the North Sea. J. Geophys. Res. Oceans 121 (3), 1529–1545.
Frederikse, T., Riva, R., Kleinherenbrink, M., Wada, Y., van den Broeke, M., Marzeion, B., 2016b. Closing the sea level budget on a regional scale: Trends and variability on the Northwestern European continental shelf. Geophys. Res. Lett. 43 (20), 10–864.
Frederikse, T., Gerkema, T., 2018. Multi-decadal variability in seasonal mean sea level along the North Sea coast. Ocean Sci. 14 (6), 1491–1501.
Fukumori, I., Wang, O., Llovel, W., Fenty, I., Forget, G., 2015. A near-uniform fluctuation of ocean bottom pressure and sea level across the deep ocean basins of the Arctic Ocean and the Nordic Seas. Prog. Oceanogr. 134, 152–172. https://doi.org/10.1016/j.pocean.2015.01.013.
Gallagher, C., Lund, R., Robbins, M., 2013. Changepoint detection in climate time series with long-term trends. J. Clim. 26 (14), 4994–5006.
Graff, J., Karunaratne, A., 1980. Accurate reduction of sea level records. The Int. Hydrographic Rev. 57 (2).
Haigh, I., Nicholls, R., Wells, N., 2009. Mean sea level trends around the English Channel over the 20th century and their wider context. Cont. Shelf Res. 29 (17), 2083–2098.
Haigh, I.D., Wahl, T., Rohling, E.J., Price, R.M., Pattiaratchi, C.B., Calafat, F.M., Dangendorf, S., 2014. Timescales for detecting a significant acceleration in sea level rise. Nat. Commun. 5, 3635.
Hames, D., Reeve, D., Marriott, M., Chadwick, A., 2004. Effect of data quality on the analysis of water levels along the cumbrian coastline. IMA International Conference on Flood Risk Assessment. University of Bath September 2004.
Hogarth, P., 2014. Preliminary analysis of acceleration of sea level rise through the twentieth century using extended tide gauge data sets (August 2014). J. Geophys. Res. Oceans 119 (11), 7645–7659. https://doi.org/10.1002/2014JC009976.
Holgate, S.J., Matthews, A., Woodworth, P.L., Rickards, L.J., Tamisiea, M.E., Bradshaw, E., Pugh, J., 2013. New data systems and products at the permanent service for mean sea level. J. Coastal Res. 29 (3), 493–504. https://doi.org/10.2112/JCOASTRES-D-12-00175.1.
Hughes, C.W., Meredith, M.P., 2006. Coherent sea-level fluctuations along the global continental slope. Philos. Trans. Royal Soc. London A: Mathematical Phys. Eng. Sci. 364 (1841), 885–901.
Killick, R., Fearnhead, P., Eckley, I.A., 2012. Optimal detection of changepoints with a linear computational cost. J. Am. Stat. Assoc. 107 (500), 1590–1598.
Kleinherenbrink, M., Riva, R., Frederikse, T., 2018. A comparison of methods to estimate vertical land motion trends from GNSS and altimetry at tide gauge stations. Ocean Sci. 14 (2).
Larsen, C.F., Echelmeyer, K.A., Freymueller, J.T., Motyka, R.J., 2003. Tide gauge records of uplift along the northern Pacific-North American plate boundary, 1937 to 2001. J. Geophys. Res. Solid Earth 108 (B4).
Lavielle, M., 2005. Using penalized contrasts for the change-point problem. Signal Process. 85 (8), 1501–1510.
Lennon, G.W., 1968. The evaluation of tide gauge performance through the van de Casteele test. Cahiers Oceanographiques 20, 867–877.
Lennon, G.W., 1971. Sea level instrumentation, its limitations and the optimisation of the performance of conventional gauges in Great Britain. Int. Hydrographic Rev. 48 (2).
Li, Y., Lund, R., 2015. Multiple changepoint detection using metadata. J. Clim. 28 (10), 4199–4216.
McCarthy, G.D., Haigh, I.D., Hirschi, J.J.M., Grist, J.P., Smeed, D.A., 2015. Ocean impact on decadal Atlantic climate variability revealed by sea-level observations. Nature 521 (7553), 508.
Nerem, R.S., Beckley, B.D., Fasullo, J.T., Hamlington, B.D., Masters, D., Mitchum, G.T., 2018. Climate-change–driven accelerated sea-level rise detected in the altimeter era. Proc. Natl. Acad. Sci. 115 (9), 2022–2025.
Peltier, W.R., Tushingham, A.M., 1989. Global sea level rise and the greenhouse effect: might they be connected? Science 244 (4906), 806–810.
Peltier, W.R., Argus, D.F., Drummond, R., 2015. Space geodesy constrains ice-age terminal deglaciation: The global ICE-6G_C (VM5a) model. J. Geophys. Res. Solid Earth 120, 450–487. https://doi.org/10.1002/2014JB011176.
Pfeffer, J., Allemand, P., 2016. The key role of vertical land motions in coastal sea level variations: a global synthesis of multisatellite altimetry, tide gauge data and GPS measurements. Earth Planet. Sci. Lett. 439, 39–47. https://doi.org/10.1016/j.epsl.2016.01.027.
Ponte, R.M., 2006. Low-frequency sea level variability and the inverted barometer effect. J. Atmos. Oceanic Technol. 23 (4), 619–629.
Pugh, D.T., 1972. The physics of pneumatic tide gauges. Int. Hydrographic Rev. 49 (2).
Pugh D.T.,1981. Comparative tests of sea level data from the Newlyn tide well and an Aanderaa pneumatic system.
Roberts, C.D., Calvert, D., Dunstone, N., Hermanson, L., Palmer, M.D., Smith, D., 2016. On the drivers and predictability of seasonal-to-interannual variations in regional sea level. J. Clim. 29 (21), 7565–7585.
Rossiter, J.R., 1967. An analysis of annual sea level variations in European waters. Geophys. J. Int. 12 (3), 259–299.
Rossiter, J.R., Gray, D.A., 1972. Sea-level observations and their secular variation. Philos. Trans. R. Soc. Lond. Series A Math. Phys. Sci. 272 (1221), 131–139.
Rude, G.T., 1926. Determination of mean sea-level at secondary stations. Am. J. Sci. 64, 312–314.
Santamaría-Gómez, A., Gravelle, M., Dangendorf, S., Marcos, M., Spada, G., Wöppelmann, G., 2017. Uncertainty of the 20th century sea-level rise due to vertical land motion errors. Earth Planet. Sci. Lett. 473, 24–32.
Suthons, C.C., 1937. The computation of mean sea level. Bulletin Géodésique 55 (1), 65–68.
Tamisiea, M.E., 2011. Ongoing glacial isostatic contributions to observations of sea level change. Geophys. J. Int. 186 (3), 1036–1044. https://doi.org/10.1111/j.1365-246X.2011.05116.x.
Teferle, F.N., Bingley, R.M., Dodson, A.H., Pna, N.T., Baker, T.F., 2002. Using GPS to separate crustal movements and sea level changes at tide gauges in the UK. In: In Vertical reference systems. Springer, Berlin, Heidelberg, pp. 264–269.
Thompson, K.R., 1980. An analysis of British monthly mean sea level. Geophys. J. Int. 63 (1), 57–73.
Thompson, K.R., 1981. The response of southern North Sea elevations to oceanographical and meteorological forcing. Estuar. Coast. Shelf Sci. 13 (3), 287–301.
Trauth, M.H., Sillmann, E. (2018) Collecting, Processing and Presenting Geoscientific Information, MATLAB and Design Recipes for Earth Sciences – Second Edition. Springer Verlag, 274 p., Supplementary Electronic Material, Hardcover, ISBN: 978-3-662-56202-4. (MDRES).
Uppala, S.M., Kållberg, P.W., Simmons, A.J., Andrae, U., Bechtold, V.D.C., Fiorino, M., et al., 2005. The ERA-40 re-analysis. Q. J. R. Meteorolog. Soc. 131 (612), 2961–3012. https://doi.org/10.1256/qj.04.176.
Volkov, D.L., Baringer, M., Smeed, D., Johns, W., Landerer, F.W., 2019. Teleconnection between the Atlantic Meridional Overturning Circulation and sea level in the Mediterranean Sea. J. Clim. 32 (3), 935–955.
Wahl, T., Haigh, I.D., Woodworth, P.L., Albrecht, F., Dillingh, D., Jensen, J., Wöppelmann, G., 2013. Observed mean sea level changes around the North Sea coastline from 1800 to present. Earth Sci. Rev. 124, 51–67.
Wakelin, S.L., Woodworth, P.L., Flather, R.A., Williams, J.A., 2003. Sea-level dependence on the NAO over the NW European Continental Shelf. Geophys. Res. Lett. 30 (7).
Walden, A.T., 1982. The statistical analysis of extreme high sea levels utilising data from the Solent. PhD Thesis. Southampton University.
Webber, N.B., Walden, A.T., 1981. Rise in mean sea level at Portsmouth. Dock and Harbour Authority 61, 385.
Whitehouse, P.L., 2018. Glacial isostatic adjustment modelling: historical perspectives, recent advances, and future directions. Earth Surf. Dyn. 6 (2), 401–429.
Williams, S.D., 2008. CATS: GPS coordinate time series analysis software. GPS Solutions 12 (2), 147–153.
Williams, S.D., Moore, P., King, M.A., Whitehouse, P.L., 2014. Revisiting GRACE Antarctic ice mass trends and accelerations considering autocorrelation. Earth Planet. Sci. Lett. 385, 12–21. https://doi.org/10.1016/j.epsl.2013.10.016.
Woodworth, P.L., 1987. Trends in UK mean sea level. Mar. Geod. 11 (1), 57–87.

Woodworth, P.L., 1991. The permanent service for mean sea level and the global sea level observing system. J. Coastal Res. 699–710.
Woodworth, P.L., Vassie, J.M., Spencer, R., Smith, D.E., 1996. Precise datum control for pressure tide gauges. Mar. Geod. 19 (1), 1–20. https://doi.org/10.1080/01490419609388068.
Woodworth, P.L., Tsimplis, M.N., Flather, R.A., Shennan, I., 1999. A review of the trends observed in British Isles mean sea level data measured by tide gauges. Geophys. J. Int. 136 (3), 651–670.
Woodworth, P.L., Smith, D.E., 2003. A one year comparison of radar and bubbler tide gauges at Liverpool. Int. Hydrographic Rev. 4 (3).
Woodworth, P.L., Teferle, F.N., Bingley, R.M., Shennan, I., Williams, S.D.P., 2009. Trends in UK mean sea level revisited. Geophys. J. Int. 176 (1), 19–30.
Woodworth, P.L., 2017. Differences between mean tide level and mean sea level. J. Geod. 91 (1), 69–90.
Wöppelmann, G., Marcos, M., 2016. Vertical land motion as a key to understanding sea level change and variability. Rev. Geophys. 54 (1), 64–92.